



# Tech Briefs

National Aeronautics and  
Space Administration



**Electronic Components and Circuits**



**Electronic Systems**



**Physical Sciences**



**Materials**



**Computer Programs**



**Mechanics**



**Machinery**



**Fabrication Technology**



**Mathematics and Information Sciences**



**Life Sciences**



# INTRODUCTION

Tech Briefs are short announcements of innovations originating from research and development activities of the National Aeronautics and Space Administration. They emphasize information considered likely to be transferable across industrial, regional, or disciplinary lines and are issued to encourage commercial application.

## Availability of NASA Tech Briefs and TSPs

Requests for individual Tech Briefs or for Technical Support Packages (TSPs) announced herein should be addressed to

### National Technology Transfer Center

Telephone No. **(800) 678-6882** or via World Wide Web at **www2.nttc.edu/leads/**

Please reference the control numbers appearing at the end of each Tech Brief. Information on NASA's Commercial Technology Team, its documents, and services is also available at the same facility or on the World Wide Web at **www.nctn.hq.nasa.gov**.

Commercial Technology Offices and Patent Counsels are located at NASA field centers to provide technology-transfer access to industrial users. Inquiries can be made by contacting NASA field centers and program offices listed below.

---

## NASA Field Centers and Program Offices

### Ames Research Center

*Carolina Blake*  
(650) 604-1754 or  
cblake@mail.arc.nasa.gov

### Dryden Flight Research Center

*Jenny Baer-Riedhart*  
(661) 276-3689 or  
jenny.baer-riedhart@dfrc.nasa.gov

### Goddard Space Flight Center

*George Alcorn*  
(301) 286-5810 or  
galcorn@gssc.nasa.gov

### Jet Propulsion Laboratory

*Merle McKenzie*  
(818) 354-2577 or  
merle.mckenzie@jpl.nasa.gov

### Johnson Space Center

*Charlene E. Gilbert*  
(281) 483-3809 or  
commercialization@jsc.nasa.gov

### John F. Kennedy Space Center

*Jim Aliberti*  
(321) 867-6224 or  
Jim.Aliberti-1@ksc.nasa.gov

### Langley Research Center

*Sam Morello*  
(757) 864-6005 or  
s.a.morello@larc.nasa.gov

### Glenn Research Center

*Larry Viterna*  
(216) 433-3484 or  
cto@grc.nasa.gov

### George C. Marshall Space Flight Center

*Vernotto C. McMillan*  
(256) 544-2615 or  
vernotto.mcmillan@msfc.nasa.gov

### John C. Stennis Space Center

*Kirk Sharp*  
(228) 688-1929 or  
technology@ssc.nasa.gov

### NASA Program Offices

At NASA Headquarters there are seven major program offices that develop and oversee technology projects of potential interest to industry:

#### Carl Ray

*Small Business Innovation Research Program (SBIR) & Small Business Technology Transfer Program (STTR)*  
(202) 358-4652 or  
cray@mail.hq.nasa.gov

#### Dr. Robert Norwood

*Office of Commercial Technology (Code RW)*  
(202) 358-2320 or  
rnorwood@mail.hq.nasa.gov

#### John Mankins

*Office of Space Flight (Code MP)*  
(202) 358-4659 or  
jmankins@mail.hq.nasa.gov

#### Terry Hertz

*Office of Aero-Space Technology (Code RS)*  
(202) 358-4636 or  
thertz@mail.hq.nasa.gov

#### Glen Mucklow

*Office of Space Sciences (Code SM)*  
(202) 358-2235 or  
gmucklow@mail.hq.nasa.gov

#### Roger Crouch

*Office of Microgravity Science Applications (Code U)*  
(202) 358-0689 or  
rcrouch@hq.nasa.gov

#### Granville Paules

*Office of Mission to Planet Earth (Code Y)*  
(202) 358-0706 or  
gpaules@mtp.e.hq.nasa.gov





**5 Electronic Components and Circuits**



**11 Electronic Systems**



**17 Physical Sciences**



**23 Materials**



**27 Computer Programs**



**31 Mechanics**



**35 Machinery**



**39 Fabrication Technology**



**43 Mathematics and Information Sciences**



**51 Life Sciences**



This document was prepared under the sponsorship of the National Aeronautics and Space Administration. Neither the United States Government nor any person acting on behalf of the United States Government assumes any liability resulting from the use of the information contained in this document, or warrants that such use will be free from privately owned rights.





# Electronic Components and Circuits

## Hardware, Techniques, and Processes

- 7 Nanoconverters for Powering Nanodevices
- 7 MOS Circuitry Would Detect Low-Energy Charged Particles
- 8 Contactless Rotary Electrical Couplings



## Nanoconverters for Powering Nanodevices

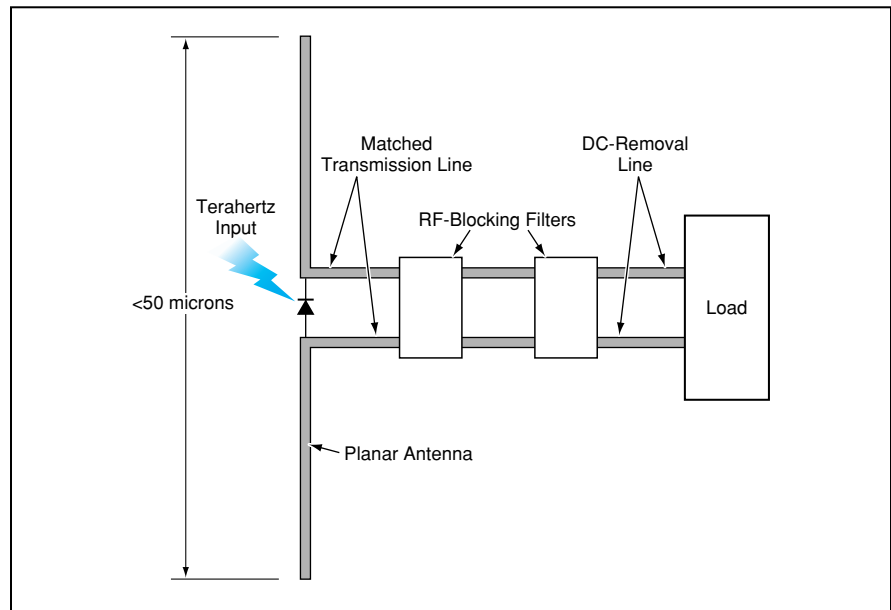
Power would be beamed at terahertz frequencies, using microscopic transmitting and receiving antennas.

NASA's Jet Propulsion Laboratory,  
Pasadena, California

Proposed integrated-circuit modules called "nanoconverters" would derive DC power from impinging electromagnetic beams having frequencies in the terahertz range. Nanoconverters are composed of microscopic antennas and diodes (see Figure 1) resembling rectennas that have been developed to perform the same function at frequencies in the gigahertz range. The submillimeter wavelength nanoconverters would make it possible to incorporate the antenna elements and diodes on structures much smaller than those of prior rectennas, thereby opening up opportunities for noncontact transmission of power to a variety of microelectronic devices, including surgically implanted medical devices and untethered microscopic robots.

The basic concept of radio beaming of electric power through space without the use of wires was explored before World War II and has been used at microwave frequencies. Novel aspects of the terahertz nanoconverter include:

1. Fully integrated monolithic rectennas at submillimeter dimensions,
2. Direct integration auto microrobots and devices,
3. Fairly high radio frequency (RF) to DC conversion efficiency with focusing optics,
4. Greater penetration in biomaterials and many plastics than infrared (IR) or visible wavelengths,
5. Negligible tissue damage due to non-



An **Antenna-and-Diode Combination** (a rectenna) would convert power from an impinging terahertz radio beam to DC. The transmission line and RF filter confine the terahertz signal to the diode and allow DC to be removed.

resonant frequencies and low beam density, and

6. Fully integrated packages for direct RF in DC out.

Techniques, processes, and equipment needed for manufacturing circuitry with dimensions comparable to those of nanoconverters have already been developed for manufacturing GaAs-based sen-

sors and sources at the frequencies. The nanoconverters could be used to remotely transmit power to microdevices in hostile environments or through smoke and dust.

*This work was done by Peter Siegel of Caltech for NASA's Jet Propulsion Laboratory. Further information is contained in a TSP [see page 1].*  
NPO-21229

## MOS Circuitry Would Detect Low-Energy Charged Particles

Conversion from ions to electrons, and photons, would not be necessary.

Metal oxide semiconductor (MOS) circuits for measuring spatially varying intensities of beams of low-energy charged particles have been developed. These circuits are intended especially for use in measuring fluxes of ions with spatial resolution along the focal planes of mass spectrometers. Unlike prior mass-spectrometer focal-plane detectors, these MOS circuits would not be based on ion-induced generation of electrons, and photons; instead, they would be based on direct detection of the electric charges of the ions. Hence, there would be no need for microchannel plates (for ion-to-electron conversion), phosphors (for electron-to-photon conversion), and photodetectors (for final

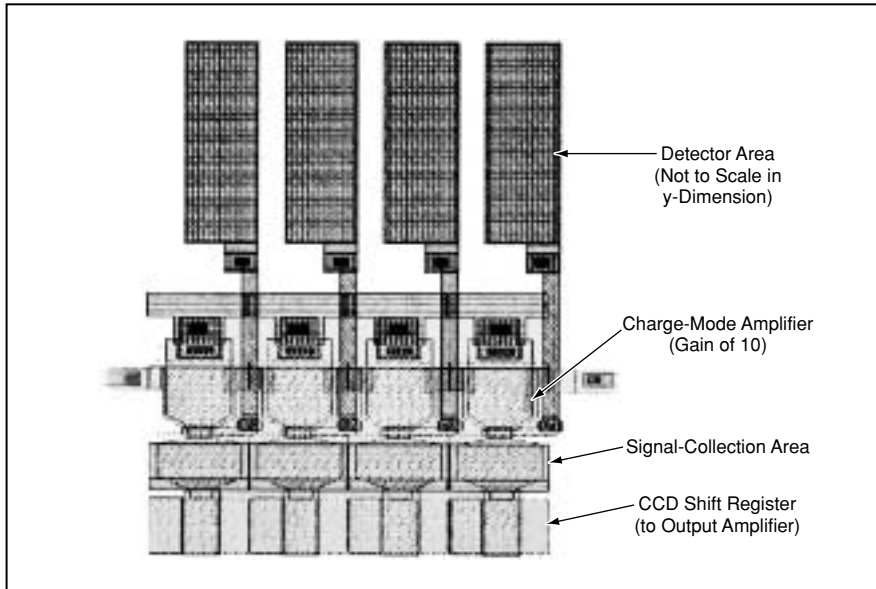
detection) — components that degrade spatial resolution and contribute to complexity and size.

The developmental circuits are based on linear arrays of charge-coupled devices (CCDs) with associated readout circuitry (see figure). They resemble linear CCD photodetector arrays, except that instead of a photodetector, each pixel contains a capacitive charge sensor. The capacitor in each sensor comprises two electrodes (typically made of aluminum) separated by a layer of insulating material. The exposed electrode captures ions and accumulates their electric charges during signal-integration periods.

The CCD array is of a standard three-

phase type. The array circuitry includes a shift register and a charge-mode input structure denoted a "fill-and-spill" structure. This structure provides the coupling through which the charge accumulated in each capacitive sensor gives rise to a packet of signal charge in the shift register. The fill-and-spill structure has previously been shown to keep the nonlinear component of response below  $-100$  dB, with negligible offset. An ancillary benefit of the fill-and-spill design is elimination of a noise component proportional to  $kTC$  (where  $k$  is Boltzmann's constant,  $T$  is absolute temperature, and  $C$  is capacitance) that would be present if the charge-storage wells in the array were to be

NASA's Jet Propulsion Laboratory,  
Pasadena, California



A Linear CCD Array contains capacitive charge sensors (instead of photodetectors) in the detector areas. Four representative pixels of the array are shown here. The detector array has many pixels (e.g., 1,024 pixels for 25-mm long array).

filled via diode sources. By appropriate design, the fill-and-spill structure can be made to provide gain in the charge domain.

The design under consideration at the time of reporting the information for this article is expected to provide a gain of 10.

The signal charges are clocked through the shift register in basically the same manner as that of a CCD photodetector array. After clocking through the array, the signal charge is presented to a charge-to-voltage-conversion output amplifier. Unlike in some CMOS photodetector circuits, there is only one such amplifier. This feature minimizes variations of signal gain and signal offset among pixels.

*This work was done by Mahadeva Sinha and Mark Wadsworth of Caltech for NASA's Jet Propulsion Laboratory. Further information is contained in a TSP [see page 1].*

*In accordance with Public Law 96-517, the contractor has elected to retain title to this invention. Inquiries concerning rights for its commercial use should be addressed to Intellectual Property group*

*JPL*

*Mail Stop 202-233  
4800 Oak Grove Drive  
Pasadena, CA 91109  
(818) 354-2240*

*Refer to NPO-21168, volume and number of this NASA Tech Briefs issue, and the page number.*

## Contactless Rotary Electrical Couplings

Efficient inductive couplings are used in place of slip rings.

*Ames Research Center,  
Moffett Field, California*

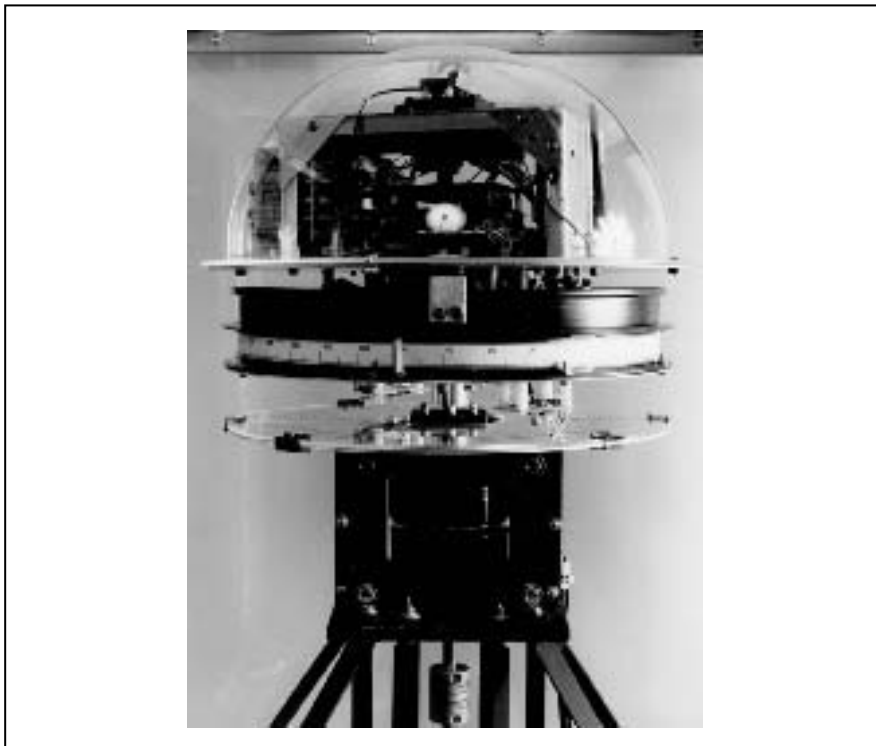


Figure 1. Transformers, Instead of Slip Rings and Brush Contacts, are used to couple ac power and data signals between stationary and rotating circuits.

Rotary electrical couplings based on induction (transformer action) rather than conduction between rotating and stationary circuitry have been invented. These couplings provide an alternative to slip rings and contact brushes.

Mechanical imperfections of slip-ring and brush contact surfaces and/or dust particles trapped between these surfaces tend to cause momentary interruptions in electrical contact and thereby give rise to electrical noise. This source of noise can be eliminated in the inductive rotary couplings because no direct contact is necessary for transformer action.

Figure 1 shows an example of the use of a rotary inductive coupling. In this application, it supplies power to a rotating digital data acquisition/transmission system test bed. The rotating data system is shown under the transparent dome and the data is transmitted via free-space optical data transmission through the dome. The rotary inductive coupling is shown in the lower half of the photograph. As in the case of conventional stationary transformers, the levels of power that can be transferred via inductive rotary couplings are limited only by con-

siderations of operating frequencies, sizes, and provisions for dissipation of heat. Typical operating frequencies for transfer of power lie in the same range as that for conventional stationary power transformers — tens to hundreds of hertz. Typical frequencies for coupling of digital data signals tend to lie at the low end of this frequency range.

Figure 2 shows a simplified cross section of a typical inductive rotary coupling between a stationary circuit and a rotating circuit mounted on a motor-driven shaft. The transformer windings comprise a stationary and a rotating coil, both concentric with the axis of rotation. Either coil can serve as the primary winding, with the other serving as the secondary winding. The stationary assembly includes a transformer core that, like a conventional stationary power transformer, is made by stacking sheets of silicon steel or other suitable magnetically "soft" material.

The transformer core partly resembles the core of a common type of conventional power transformer; it includes an inner part framed in a generally rectangular outer part. However, unlike the core of a conventional power transformer, this core includes a clearance hole for the rotating shaft, and the inner core is a round cylinder (instead of a rectangular solid) with the clearance hole lying along its axis. Moreover, there is a gap at one end of the inner core to provide clearance for a clamp that attaches the rotating coil to the shaft. Both coils are annular, with inner radii and outer radii to fit the recess between the inner and outer core. To provide clearance for rotation, the inner radius of the stationary coil must be made somewhat greater than the outer radius of the inner part of the core.

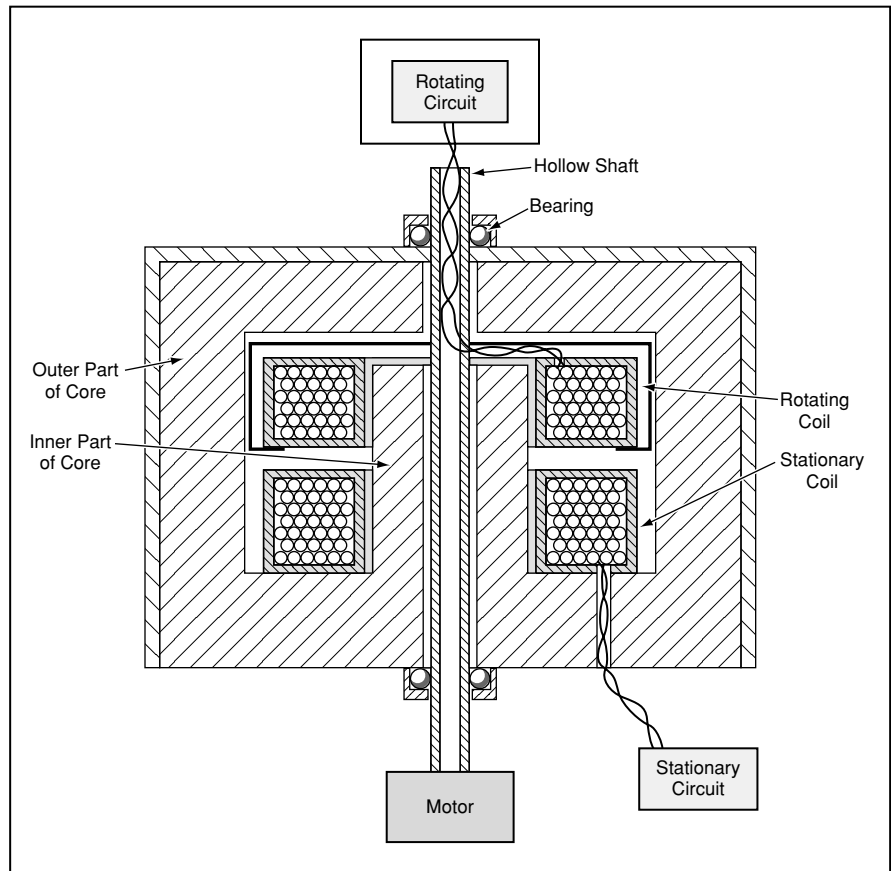


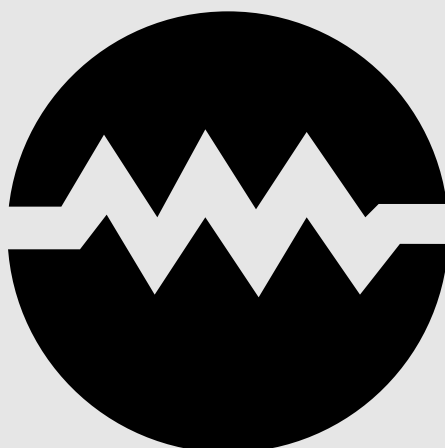
Figure 2. This **Inductive Rotary Coupling** resembles a conventional stationary transformer, except that one coil rotates with a shaft that passes through the middle, and the core is shaped to accommodate the rotating parts. The hollow shaft accommodates the wires that connect the rotating coil with the rotating circuit at one end of the shaft.

*This work was done by Hiroyuki Kumagai of Aerospace Computing, Inc., for **Ames Research Center**. Further information is contained in a TSP [see page 1].*

*This invention has been patented by NASA (U.S. Patent No. 5,691,687). Inquiries*

*concerning nonexclusive or exclusive license for its commercial development should be addressed to the Patent Counsel, Ames Research Center [see page 1]. Refer to ARC-12072.*





# Electronic Systems

## Hardware, Techniques, and Processes

- 13 Optoelectronic System for Measuring Heights Above a Floor
- 14 Signal-Conditioning Amplifier Recorders
- 15 Integrated Optoelectronics for Parallel Microbioanalysis
- 15 Relating Downlink Data Products to Uplink Commands



# Optoelectronic System for Measuring Heights Above a Floor

One technician can take measurements that previously involved four workers.

John F. Kennedy Space Center,  
Florida

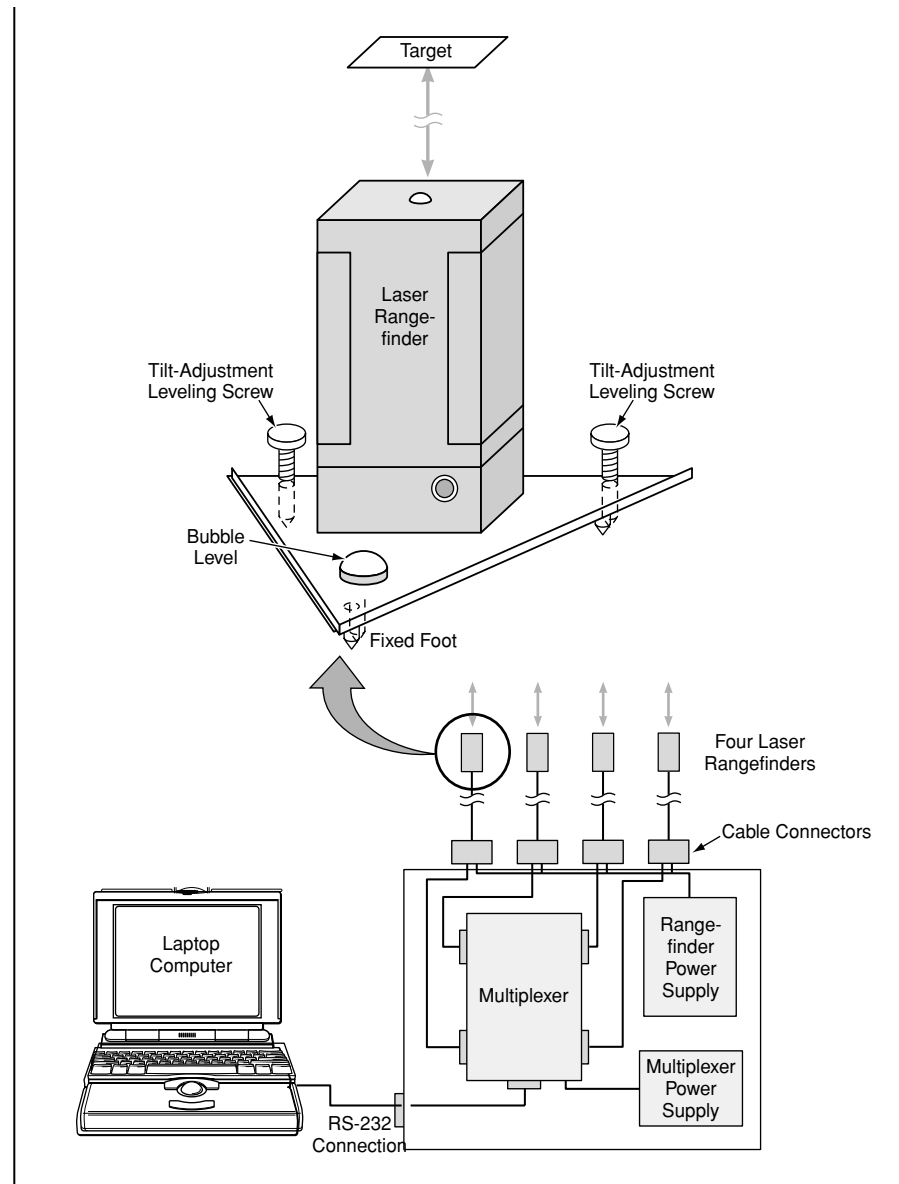
An optoelectronic system has been developed for measuring heights, above a floor, of designated points on a large object. In the original application for which the system was conceived, the large object is a space shuttle and the designated points are two front and two rear points for the attachment of jacks for positioning the shuttle at the height and horizontal pitch specified for maintenance operations. The front and rear jacking points are required to be raised to heights of  $198 \pm 1/4$  in. ( $502.9 \pm 0.6$  cm) and  $120.6 \pm 1/4$  in. ( $306.4 \pm 0.6$  cm), respectively.

Prior to the development of this system, the measurement for each jacking point involved an error-prone, time-consuming procedure in which two technicians were needed to position two telescoping rods with graduations of  $1/16$  in. (1.6 mm.), an inspector was needed to ensure that the rods were vertical, and the technicians reported the readings to a fourth person who directed the jacking and leveling from a position 30 to 40 ft (9 to 12 m) away. In contrast, the present system can be operated by one person, and once the initial setup of the system has been completed, the system performs and processes the height measurements quickly on command.

The system (see figure) is based on the use of laser rangefinders to measure the heights. As such, it bears some similarity to the laser-rangefinder-based systems described in "Apparatus and Technique for Measuring Distance Between Axles" (KSC-11980) *NASA Tech Briefs*, Vol. 24, No. 3 (March 2000), page 76 and "Using Laser Rangefinders To Align Two Structures" (KSC-12040) *NASA Tech Briefs*, Vol. 25, No. 1 (January 2001), page 16a.

Each laser rangefinder is mounted on a triangular platform that is placed on the floor below one of the jacking points. The laser rangefinder is aimed upward at a target attached temporarily to the jacking point. The platform is equipped with tilt-adjustment screws and a bubble level to enable correction for any deviation of the floor from flatness. The bubble level is accurate to  $\pm 0.2^\circ$  — well within the applicable tolerance of  $\pm 2^\circ$  corresponding to a height error of  $\pm 1/8$  in. (0.3 cm).

The four laser rangefinders are connected via cables to a multiplexer located in an electronic enclosure. The multiplexer enables serial data communications between the



**Four Laser Rangefinders Measure the Heights** of four jacking points above a floor. The rangefinders are controlled and monitored via a computer. A complete measurement cycle takes less than three seconds.

laser rangefinders and a laptop computer. The computer is programmed with special-purpose software for controlling the rangefinders and the multiplexer.

The software generates a graphical display containing an image of the space shuttle with vertical bars superimposed at the jacking points to represent the heights. The height readings are displayed numerically. Each bar is also color-coded: green if the height is within tolerance and either yellow,

steady red, or flashing red, depending on the sign and magnitude of the deviation from tolerance. The nominal values, tolerances, and/or other height values for triggering the various colors can be set by use of a normally hidden menu in the computer display. Typically, the system takes less than 3 seconds to perform all four distance measurements and process them into the display. In the event of failure of one of the rangefinders, the software generates a "data drop out"

message instead of displaying the corresponding height measurement and color.

This work was done by Robert C. Youngquist (formerly of Dynacs) and Chris

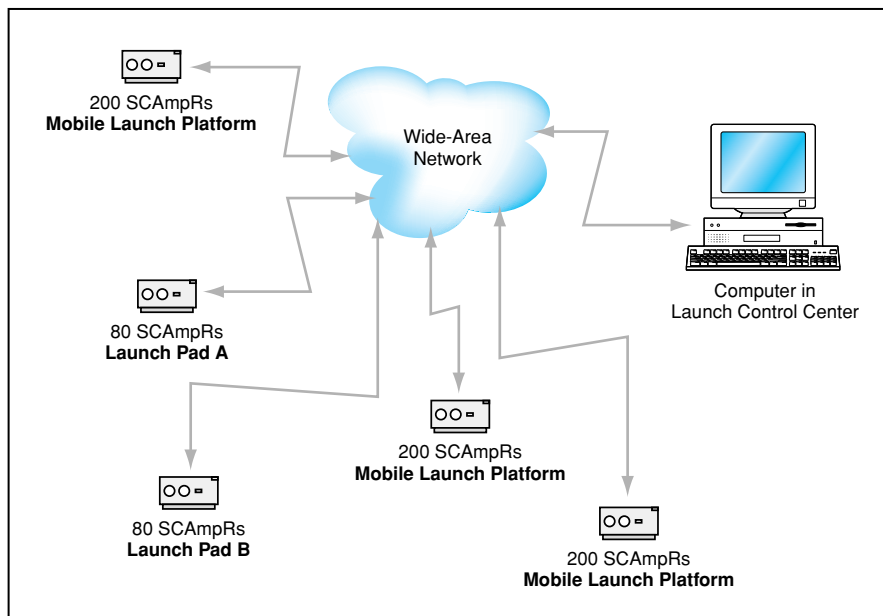
Davis of Kennedy Space Center; Jimmy Polk, Brad Burns, William Haskell, and Tim Opalka of Dynacs Engineering Co., Inc; and Michael McClure of United Space Alliance.

Further information is contained in a TSP [see page 1].  
KSC-12098

## Signal-Conditioning Amplifier Recorders

The cost and complexity of a data-acquisition system would be reduced.

John F. Kennedy Space Center,  
Florida



**Data Would Be Recorded Temporarily by the SCAMP-Rs** and later transmitted to the computer in the launch control center via the wide-area network. This arrangement is less complex than is that of the present system, in which the data are transmitted to redundant recording equipment via a redundant and more complex system of communication links and interfaces.

Signal-conditioning amplifier recorders (SCAMP-Rs) have been proposed as a means of simplifying and upgrading the Kennedy Space Center (KSC) Ground Measurement System (GMS), which is a versatile data-acquisition system that gathers and records a variety of measurement data before and during the launch of a space shuttle. In the present version of the GMS system, signal conditioning amplifiers digitize and transmit data to a VME chassis that multiplexes up to 416 channels. The data is transmitted via a high-speed data bus to a second VME chassis where it is available for snapshots. The data is passed from the second VME chassis to a high-speed data recorder. This process is duplicated for installations at two launch pads and the Vehicle Assembly Building (VAB). Since any failure of equipment in the data path results in loss of data, much of the system is redundant. The architecture of the existing GMS limits expansion or any modification to the system to meet changing requirements because of the cost and time required. A SCAMP-R-based system is

much more flexible.

The basis of the simplification, flexibility, and reliability is the shifting of the recording function to the individual amplifier channels. Each SCAMP-R is a self-contained single channel data acquisition system, which in its current implementation, has a data storage capacity of up to 30 minutes when operating at the fastest data sampling rates. The SCAMP-R channels are self-configuring and self-calibrating. Multiple SCAMP-R channels are ganged on printed circuit boards and mounted in a chassis that provides power, a network hub, and Inter-Range Instrument Group (IRIG) time signals. The SCAMP-R channels share nothing except physical mounting on a circuit board. All circuitry is electrically separate for each channel. All that is necessary to complete the data acquisition system is a single master computer tied to the SCAMP-R channels by standard network equipment. The size of the data acquisition system dictates the requirements for the specific network equipment.

The computer polls each channel for health status and data snapshots. The

bandwidth of the network dictates the extent of the data snapshots. It is likely that in most applications the health status/data snapshot frame can be obtained often enough to pass all data in real time to the master computer. Data is time tagged and stored safely in non-volatile memory at the SCAMP-R where it remains for retrieval regardless of the status of the communication network. Once a SCAMP-R is commanded to record, no further communication is necessary to successfully complete a measurement. Even the loss of the IRIG time input will not cause a disruption because each SCAMP-R channel will automatically revert to generating time if the input is interrupted.

A SCAMP-R can record data in any of a variety of ways upon command. For example:

- A SCAMP-R can be configured to record and time-stamp data only when a pre-defined minimum change occurs, for example during a long fueling operation where flows and pressures would normally remain constant.
- A SCAMP-R can be commanded to start recording at a future time, for a given duration, so that in the event of a failure of communication at a critical time, data would still be recorded as originally intended. As long as communication continued, the commanded starting time could be adjusted (as would be needed to accommodate a hold in the launch countdown).
- A SCAMP-R can be commanded to record data samples at a specified rate or to sample at different specified rates at specified times in the future.

Inexpensive commercial-off-the-shelf (COTS) hubs integrate the SCAMP-R chassis into a communications network. Transfer of data and other communications, such as commands and health status, will be performed by a standard method of network communication. The current implementation is a polling form of TCP/IP. Any number of computers can be connected to the network for viewing or rebroadcasting of data snapshots in addition to commanding and monitoring health status of the SCAMP-R channels.

The GMS is intended to be a quick response system. A SCAMP chassis can be installed for special situation measurements with minimal infrastructure requirements. Also, it has become a recurring requirement for the GMS to support measurements during rollout of the mobile launch platform. The SCAMP architecture

will provide the capability for quick implementation of a very reliable and easily reconfigurable data acquisition system.

*This work was done by Pedro J. Medelius and John Taylor of Dynacs, Inc., for Kennedy Space Center. Further information is contained in a TSP [see page 1].*

*This invention is owned by NASA, and a*

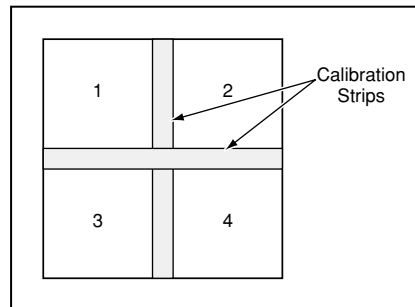
*patent application has been filed. Inquiries concerning nonexclusive or exclusive license for its commercial development should be addressed to the Technology Programs and Commercialization Office, Kennedy Space Center, (321) 867-8130. Refer to KSC-12296.*

## Integrated Optoelectronics for Parallel Microbioanalysis

Tests for microbial species and hazardous chemicals could be performed quickly and inexpensively.

Miniature, relatively inexpensive microbioanalytical systems ("laboratory-on-a-chip" devices) have been proposed for the detection of hazardous microbes and toxic chemicals. Each system of this type would include optoelectronic sensors and sensor-output-processing circuitry that would simultaneously look for the optical change, fluorescence, delayed fluorescence, or phosphorescence signatures from multiple redundant sites that have interacted with the test biomolecules in order to detect which one(s) was present in a given situation. These systems could be used in a variety of settings that could include doctors' offices, hospitals, hazardous-material laboratories, biological-research laboratories, military operations, and chemical-processing plants.

Each system would consist primarily of an integrated circuit or perhaps several integrated circuits packaged together. The system would include (1) a source of optical excitation (e.g., ambient light, superluminescent or laser diode); (2) a photodetector-array circuit of the active-pixel-sensor (APS) type that would be compatible with complementary metal oxide semiconductor (CMOS) circuitry; and (3) on-chip signal-and data-processing circuits for rapid and reliable identification of toxic substances and biomolecules (e.g., antigens) associated with known or general classes of hazardous chemicals, bacteria, and viruses. Each pixel or group of pixels in the APS array would be coated with an antigen-specific optobiochemical reagent or other substance that would change its resultant



In this **Simplified Example of a Biomolecular-Signature Detector** with self-calibration, the APS array would be divided into four pixels or groups of pixels, each coated with a different substance that would act as a receptor for one of four fluorophores associated with one of four molecules that one seeks to detect.

optical characteristics (i.e., absorption, fluorescence, luminescence, etc.) in response to a biomolecule or hazardous chemical that one seeks to identify. In addition, the array could include strips, bonded directly to the APS surface (see figure), that would produce known temporal and spectral APS outputs for on-chip or off-chip calibration.

In the use of a system of this type, unlike in conventional bioanalytical laboratory practice, the detection of biohazards would not be subject to the limits of visual acuity of human observers and of the resolution of conventional microscopes. Moreover, detection would not be slowed by the need to perform repetitive tedious procedures under sterile laboratory conditions. Instead, it would be possible to simultaneously identify any or all of a large number of different microbial species and/or chemical agents

*NASA's Jet Propulsion Laboratory,  
Pasadena, California*

within an analysis time of a few seconds. For example, the number of species and/or chemical agents that could be identified could be as large as a million in the case of a 1,024-by-1,024-pixel APS array.

In a typical analytical procedure, a sample would be dissolved or otherwise suspended in a transport liquid, whereby liquid would be deposited onto the surface of the APS array. After a specified interaction time, the light source (ambient or pulsed) would be sensed and the APS array would be gated so as not to respond to the source light but to respond to the longer-lived fluorescence that would follow the source pulses. The intensity change and/or delayed fluorescence signal from each pixel would be read out and analyzed; the analysis of the signal from each pixel could include correlation with calibration signals and/or with signals from other pixels. In a case in which the response from a pixel could include optical or fluorescence signatures from multiple bioanalytical or fluorescent probes associated with different target molecules of interest, it would be possible to distinguish among them by their position and/or fluorescence lifetimes. For the purpose of measuring fluorescence lifetimes, the light source could be modulated periodically and the reading from each pixel taken at multiple fixed phase delays relative to the optical excitation.

*This work was done by Robert Stirbl, Philip Moynihan, Gregory Bearman, and Arthur Lane of Caltech for NASA's Jet Propulsion Laboratory. Further information is contained in a TSP [see page 1].*  
NPO-21047

## Relating Downlink Data Products to Uplink Commands

Data returned by exploratory robots are associated with previously issued commands.

An improved data-labeling system provides for automatic association of data products of an exploratory robot (downlink information) with previously transmitted

commands (uplink information) that caused the robot to gather the data. Such association is essential to correct and timely analysis of the data products — including, for

*NASA's Jet Propulsion Laboratory,  
Pasadena, California*

example, association of the data with the correct targets. The system was developed for use on Mars Rover missions during the next few years. The system could also be

adapted to terrestrial exploratory telerobots for which delays between commands and data returns are long enough to give rise to questions as to which commands resulted in which data returns. The main advantage of this system over prior data-labeling systems is that given a downlink data product, the uplink command and sequence hierarchy that produced it are automatically provided, and given an uplink sequence and command, the downlink data products that it produced are automatically provided.

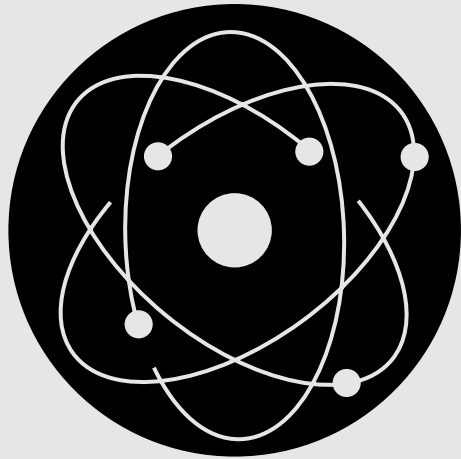
The system was demonstrated during a field test using the Field Integrated Design and Operations (FIDO) rover, which is a prototype Mars-exploration mobile robot used as an operations test bed for the NASA 2003 Mars Exploration Rover (MER) mission, which is scheduled to land two rovers

on Mars in early 2004. A sequence identifier is uplinked along with each sequence of commands. Aboard the rover, a command is incremented each time a command is executed, and both the sequence identifier and the current command count are downlinked along with each data product generated pursuant to the command. Thereafter, sequence identifiers and command counts are used as indices for relating commands with data products in the processing and storage of the data products and in the automated generation of Hypertext Markup Language (HTML) reports. An automatically-generated HTML report system allows a user to browse through and view the resulting data products as indexed by the sequence and command hierarchy that produced them. During the downlink process-

ing step for each data product, the uplink sequence hierarchy, i.e., command, target, macro, request, and sequence, that produced it are stored with the data product. Then operations software tools can provide this uplink sequence information with each data product. This has been implemented in the Web Interface for Telescience (WITS) rover operations tool, which has been described in prior *NASA Tech Briefs* articles.

*This work was done by Paul Backes, Jeffrey Norris, and Mark Powell of Caltech for **NASA's Jet Propulsion Laboratory**. Further information is contained in a TSP [see page 1].*

*This software is available for commercial licensing. Please contact Don Hart of the California Institute of Technology at (818) 393-3425. Refer to NPO-30416.*



# Physical Sciences

## Hardware, Techniques, and Processes

- 19 Pulsed-Source Interferometry in Acoustic Imaging
- 19 Thermo-Electron Ballistic Coolers or Heaters
- 20 Optoelectronic Apparatus Measures Glucose Noninvasively
- 21 Floating Probe Assembly for Measuring Temperature of Water
- 22 Proton Collimators for Fusion Reactors



## Pulsed-Source Interferometry in Acoustic Imaging

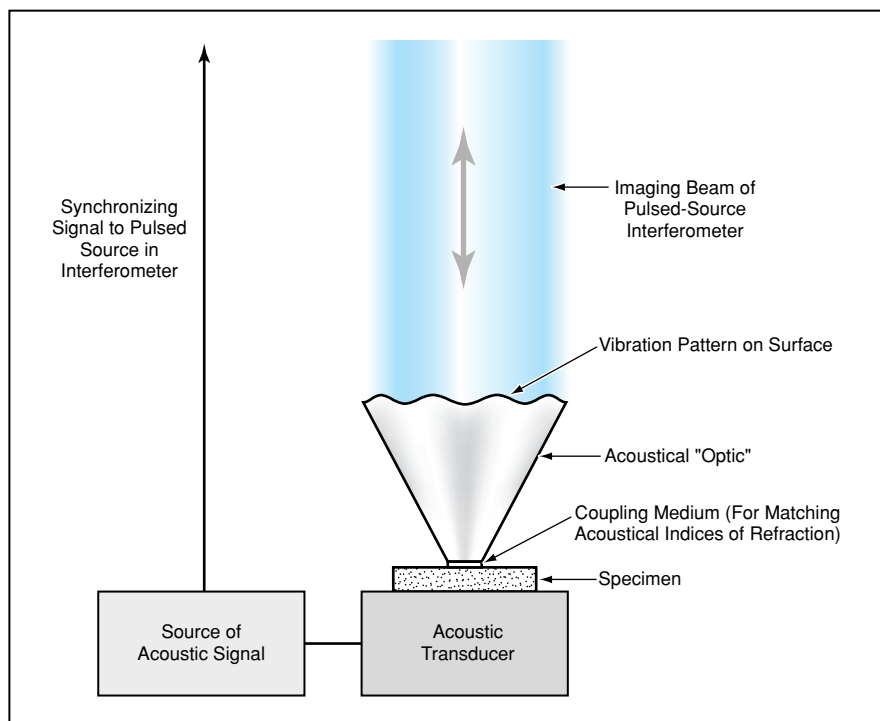
Buried features as small as 30 nm could be resolved.

NASA's Jet Propulsion Laboratory,  
Pasadena, California

A combination of pulsed-source interferometry and acoustic diffraction has been proposed for use in imaging sub-surface microscopic defects and other features in such diverse objects as integrated-circuit chips, specimens of materials, and mechanical parts. A specimen to be inspected by this technique would be mounted with its bottom side in contact with an acoustic transducer driven by a continuous-wave acoustic signal at a suitable frequency, which could be as low as a megahertz or as high as a few hundred gigahertz (see figure). The top side of the specimen would be coupled to an object that would have a flat (when not vibrating) top surface and that would serve as the acoustical analog of an optical medium (in effect, an acoustical "optic").

Microfeatures within the specimen would diffract the acoustic wave. The diffracted wave would propagate through the acoustical "optic," forming a vibration pattern on the top surface. The vibration pattern would be measured twice by use of a pulsed-source optical interferometer; the first measurement would be taken in phase, the second 90° out of phase with the acoustic signal at its source. The amplitude and phase of the vibration pattern, and thus of the acoustic field, would be computed from the two measurements. Then by use of a diffraction formula, the acoustic pattern would be computationally propagated back into the specimen to obtain an acoustic image of the internal microfeatures.

The pulsed-source interferometer has already been demonstrated, in a different application, to afford an amplitude resolu-



**A Pulsed-Source Interferometer** would be used to measure the phase and amplitude of a vibration pattern related to acoustic diffraction by microfeatures in the specimen. The pattern would then be used to compute an acoustic image of the microfeatures.

tion as small as 1 nm. With refinements in design and operation, it should be possible to resolve amplitudes an order of magnitude smaller. If, in addition, the acoustic frequency were at least 30 GHz, then it should be possible to image features as small as 30 nm. The ability to image at such high resolution would be a significant contribution to the art of nondestructive microscopy. Of course, lower acoustic fre-

quencies could be used to image larger features in applications in which the highest resolution is not needed.

*This work was done by Kirill Shcheglov, Roman Gutierrez, and Tony K. Tang of Caltech for NASA's Jet Propulsion Laboratory. Further information is contained in a TSP [see page 1].*  
NPO-20478

## Thermo-Electron Ballistic Coolers or Heaters

These devices may surpass currently available thermoelectric devices.

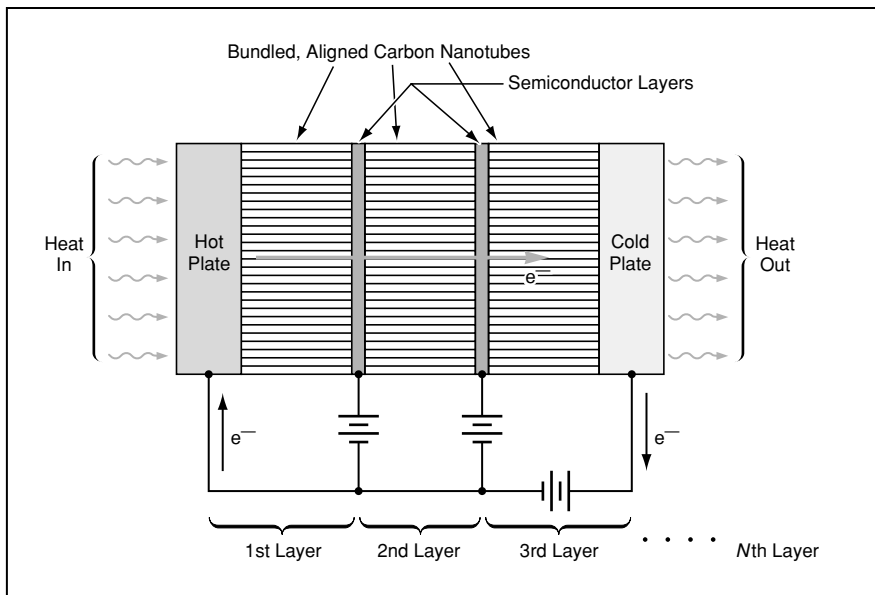
Langley Research Center,  
Hampton, Virginia

Electronic heat-transfer devices of a proposed type would exploit some of the quantum-wire-like, pseudo-superconducting properties of single-wall carbon nanotubes or, optionally, room-temperature-superconducting polymers (RTSPs). The devices are denoted thermo-electron ballistic (TEB) coolers or heaters because one of the properties that they exploit is the totally or nearly ballistic (dissipation or scattering free) transport of electrons. This property is observed in RTSPs and carbon nanotubes that are

free of material and geometric defects, except under conditions in which oscillatory electron motions become coupled with vibrations of the nanotubes. Another relevant property is the high number density of electrons passing through carbon nanotubes — sufficient to sustain electron current densities as large as 100 MA/cm<sup>2</sup>. The combination of ballistic motion and large current density should make it possible for TEB devices to operate at low applied potentials while pumping heat at rates sev-

eral orders of magnitude greater than those of thermoelectric devices. It may also enable them to operate with efficiency close to the Carnot limit. In addition, the proposed TEB devices are expected to operate over a wider temperature range.

A typical TEB device (see figure) would include an electrically and thermally conductive plate, denoted the hot plate, on the side from which heat is to be transferred;  $N$  layers ( $N = 3$  in the figure) of bundled and aligned carbon nanotubes interspersed



**0A TEB Device** would exploit thermionic emission, ballistic transport of electrons in carbon nanotubes, and Schottky barriers at nanotube/semiconductor interfaces. The thickness of each nanotube layer would be of the order of 5  $\mu\text{m}$ .

with  $N - 1$  semiconductor layers; an electrically and thermally conductive plate, denoted the cold plate, on the side to which heat is to be transferred; and small batteries or other DC electric power sources and wiring connected to the hot and cold plates and to the semiconductor layers. Under the influence of the electric potential field applied by the DC sources, some of the thermally agitated electrons would be adiabatically swept away from the hot plate into the first layer of nanotubes. (Because of this mode of operation, the device could also be called a

thermionic cooler or heater.) The applied electric field would accelerate the electrons moving in the nanotubes, giving them enough kinetic energy to overcome the Schottky barrier at the nanotube/semiconductor interface. Consequently, the Schottky barrier would act as a one-way valve for energetic electrons.

In the same manner as described above, thermally agitated electrons in each semiconductor layer would be made to travel through the next nanotube layer to the next semiconductor layer, and so forth until the

electrons reach the cold plate, from whence they would be removed via an ohmic contact into the wiring. The closed electric circuit would maintain charge neutrality, supplying electrons to the hot plate and semiconductor layers to replace those removed by thermionic emission and applied electric fields. In addition to a DC potential applied between the hot and cold plates, DC bias potentials could be applied to the semiconductor layers to control the quantum-mechanical tunneling of electrons through the Schottky barriers.

It will be necessary to perfect a number of techniques in order to fabricate TEB devices. Among these are techniques for (1) depositing RTSPs or growing highly pure, aligned single-wall carbon nanotubes on electrically and thermally conductive substrates that can serve as hot and cold plates; (2) cutting the nanotubes to make clean, flat planes on which semiconductor layers can be deposited; and (3) depositing RTSPs or growing highly pure, aligned single-wall carbon nanotubes on the semiconductor layers. The overall thickness of a TEB device would be determined largely by the number of carbon-nanotube layers, the length ( $\approx 5 \mu\text{m}$ ) of the nanotubes in each layer, and the thicknesses of the semiconductor layers. It should be possible to make TEB devices so thin that they could be incorporated into or onto flexible structures.

*This work was done by Sang H. Choi of Langley Research Center. Further information is contained in a TSP [see page 1]. LAR-16222*

## Optoelectronic Apparatus Measures Glucose Noninvasively

The concentration of glucose is obtained through a combination of interferometry and polarimetry.

An optoelectronic apparatus has been invented as a noninvasive means of measuring the concentration of glucose in the human body. The apparatus performs polarimetric and interferometric measurements of the human eye to acquire data from which the concentration of glucose in the aqueous humor can be computed. Because of the importance of the concentration of glucose in human health, there could be a large potential market for instruments based on this apparatus.

The apparatus (see figure) includes a light source equipped with a linear polarizer and a quarter-wave retarder to generate a beam of circularly polarized light. The beam is aimed at an eye at an angle of incidence ( $\theta$ ) chosen so that after refraction at the surface

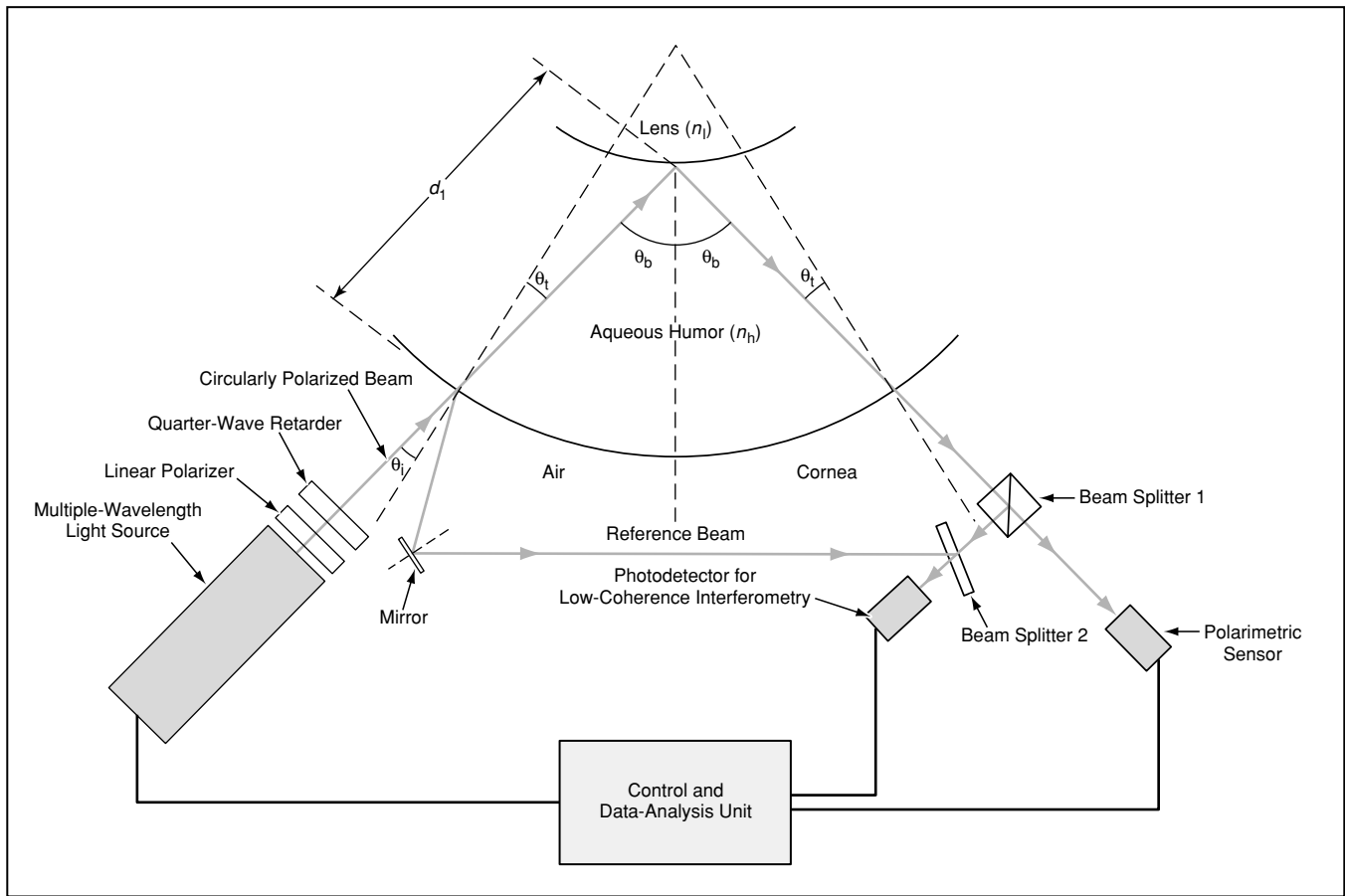
of the cornea, it travels through the aqueous humor and impinges on the crystallin lens at the Brewster angle [ $\theta_b = \arctan(n_l/n_h)$ , where  $n_l$  and  $n_h$  are the indices of refraction of the lens and the aqueous humor, respectively]. The portion of the beam that enters and passes through the eye is denoted the probe beam. The portion of the beam reflected from the cornea is further reflected by a mirror and used as a reference beam for low-coherence interferometry.

The Brewster-angle arrangement causes the portion of the probe beam reflected from the lens to be linearly polarized perpendicular to the plane of incidence (which here coincides with the plane of the page). As the reflected probe beam traverses the aqueous humor, glucose molecules rotate its plane of

*John H. Glenn Research Center, Cleveland, Ohio*

polarization. This rotational effect is well established: It is characterized by previously determined, wavelength-dependent proportionality between (1) the angle of rotation of the plane of polarization and (2) the product of the concentration of glucose and the length of the optical path through the solution (in this case, aqueous humor) that contains the glucose. Hence, if one can measure the rotation of polarization of the reflected light and the length of its path through the aqueous humor, one can calculate the concentration of glucose by use of the aforementioned proportionality.

After leaving the eye, the reflected probe beam enters beam splitter 1. Part of the probe beam passes through beam splitter 1 and goes to a polarimetric sensor, which



**Light Beams Are Reflected and Transmitted** by several components of the eye. The polarimetric and interferometric properties of the reflected and transmitted beams contain information on the concentration of glucose in the aqueous humor.

measures its angle of polarization. From this angle and the known orientation of the plane of incidence on the lens, the rotation angle can be determined. Part of the probe beam leaving the eye is reflected from beam splitter 1 toward beam splitter 2, wherein it is combined with the reference beam. The combination of the probe reference beams impinges on a photodetector for use in low-coherence interferometry to measure the total length of the path of the probe beam through the aqueous humor. By virtue of symmetry, half of this path length contributes to the measured rotation and is, therefore,

the length to use in calculating the concentration of glucose.

As described thus far, the principle of operation does not necessarily involve the use of multiple wavelengths. The value of multiwavelength operation lies in the possibility of compensating for rotation caused by analytes other than glucose. By measuring at a number of wavelengths equal to the number of analytes (including glucose) that contribute to rotation and knowing the wavelength-dependent specific rotation, one can solve the system of linear equations for the rotation at the various wavelengths to

extract the concentration of glucose (and, incidentally, of the other analytes).

*This work was done by Rafat R. Ansari of Glenn Research Center and Luigi L. Rovati of the University of Brescia. Further information is contained in a TSP [see page 1].*

*Inquiries concerning rights for the commercial use of this invention should be addressed to NASA Glenn Research Center, Commercial Technology Office, Attn: Steve Fedor, Mail Stop 4-8, 21000 Brookpark Road, Cleveland, Ohio 44135. Refer to LEW-17216.*

## Floating Probe Assembly for Measuring Temperature of Water

Temperatures are measured at several depths.

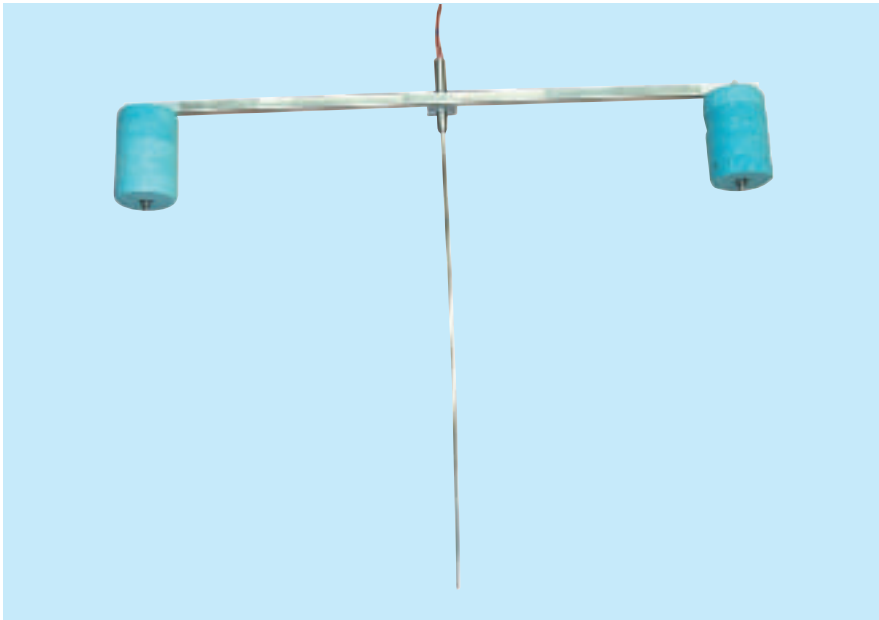
A floating apparatus denoted a temperature probe aquatic suspension system (TPASS) has been developed for measuring the temperature of an ocean, lake, or other natural body of water at predetermined depths. These types of measurements are used in computer models to relate remotely

sensed water-surface temperature to bulk-water temperature. Prior instruments built for the same purpose were found to give inaccurate readings because the apparatuses themselves significantly affected the temperatures of the water in their vicinities. The design of the TPASS is intended to satisfy a

requirement to minimize the perturbation of the temperatures to be measured.

The TPASS (see figure) includes a square-cross-section aluminum rod 28 in. ( $\approx 71$  cm) long with floats attached at both ends. Each float includes five polystyrene foam disks about 3/4 in. ( $\approx 1.9$  cm) thick and

*Stennis Space Center,  
Mississippi*



This **Temperature-Probe Assembly** floats on a body of water. The metal sleeve at the middle hangs down into the water. Temperature probes are mounted inside the sleeve for measuring temperatures at several different depths.

2.5 in. ( $\approx 6.4$  cm) in diameter. The disks are stacked to form cylinders, bolted to the rod, and covered with hollow plastic sleeves. A metal sleeve is clamped to the middle of the aluminum rod, from whence it hangs down into the water. Temperature probes (which can be thermocouples, thermistors, or resistance temperature devices) are placed within the sleeve at the desired measurement depths. Wires from the temperature probes are routed to the input terminals of a data logger.

*This work was done by Randy Stewart of Lockheed Martin Corp. and Clyde Ruffin of GB Tech, Inc., for Stennis Space Center. Further information is contained in a TSP [see page 1].*

*Inquiries concerning rights for the commercial use of this invention should be addressed to the Intellectual Property Manager, Stennis Space Center [see page 1]. Refer to SSC-00136.*

## Proton Collimators for Fusion Reactors

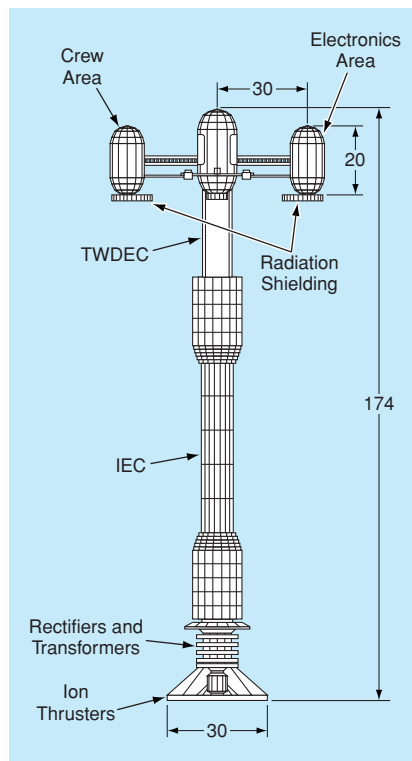
High-energy protons would be channeled into useful beams.

Proton collimators have been proposed for incorporation into inertial-electrostatic-confinement (IEC) fusion reactors. Such reactors have been envisioned as thrusters and sources of electric power for spacecraft and as sources of energetic protons in commercial ion-beam applications. An artist's concept for an IEC powered spaceship designed for round trip missions to Mars and Jupiter is shown in the figure.

An IEC fusion reactor typically contains a plasma of pure  $^2\text{H}$  or a  $^2\text{H}$ - $^3\text{He}$  mixture. Collisions among the  $^2\text{H}$  and/or  $^3\text{He}$  nuclei give rise to fusion reactions, the main energetic products of which are protons with kinetic energy  $\approx 14$  MeV and an isotropic velocity distribution. A proton collimator would collect the isotropically emitted protons and form them into a collimated beam.

A proton collimator would include (1) an electromagnet outside the fusion reactor that would impose a substantially uniform magnetic field within the reactor and (2) a pair of electromagnet coils inside the reactor, oriented to generate magnetic fields antiparallel to the one generated by the external electromagnet. The interior electromagnet coils would be positioned so that the fusion reaction would be concentrated in a region between them. The currents in the interior electromagnet coils would be adjusted to minimize the net magnetic field in the fusion-reaction region in order to avoid adverse

*Marshall Space Flight Center,  
Alabama*



A scale schematic of **100-MWe IEC Fusion-Powered Spacecraft** is depicted with dimensions in meters. (Note TWDEC = Traveling-Wave Direct Energy Converter.)

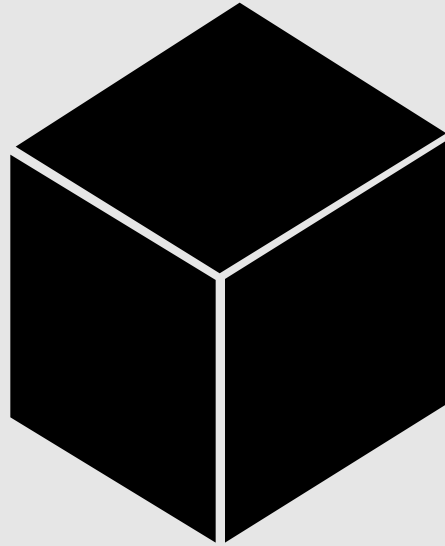
effect of the magnetic field on the trajectories of the  $^2\text{H}$ - $^3\text{He}$  ions that must collide to cause

fusion reactions. The accessible region for the ions and electrons can be completely separated from inner electromagnet coils and support the structure, preventing bombardment damage.

The overall effect of the electromagnets would be to channel the isotropically emitted 14-MeV protons into a beam substantially parallel to the magnetic field. The collimator would also separate the 14-MeV protons from unreacted fuel ions leaking out of the reaction region. The leaking fuel constituents would be collected on plates, condensed to a gas, pumped out, and recycled to the reactor.

The collimated proton beam could be used directly for spacecraft thrust or an industrial ion-beam application. Alternatively, the proton collimator would be used in conjunction with a magnetic expander and an electron/ion separator to generate a net electric current. Another approach under consideration for space propulsion is to focus the beam on a target, e.g., a small plastic pellet, which would be vaporized and exhausted through a magnetic nozzle. Yet another alternative is to introduce the beam into a highly efficient traveling-wave energy-conversion device to extract electric power.

*This work was done by George H. Miley and Hiromu Momota of NPL Associates, Inc., for Marshall Space Flight Center. Further information is contained in a TSP [see page 1]. MFS-31734*



# Materials

## Hardware, Techniques, and Processes

- 25 Low-Power RIE of  $\text{SiO}_2$  in  $\text{CHF}_3$  To Obtain Steep Sidewalls
- 25 Annealing Would Improve  $\beta''$ —Alumina Solid Electrolyte



## Low-Power RIE of SiO<sub>2</sub> in CHF<sub>3</sub> To Obtain Steep Sidewalls

Process parameters are chosen carefully to minimize deleterious effects.

A reactive-ion etching (RIE) process has been developed to enable the formation of holes with steep sidewalls in a layer of silicon dioxide that covers a silicon substrate. The holes in question are through the thickness of the SiO<sub>2</sub> and are used to define silicon substrate areas to be etched or to be built upon through epitaxial deposition of silicon. The sidewalls of these holes are required to be vertical in order to ensure that the sidewalls of the holes to be etched in the substrate or the sidewalls of the epitaxial deposits, respectively, also turn out to be vertical.

The pattern of holes in the SiO<sub>2</sub> mask is established by use of a photoresist mask on top of the SiO<sub>2</sub>. The holes in the photoresist mask must also have vertical sidewalls. Prior techniques for etching the SiO<sub>2</sub> areas exposed through the holes in the photoresist mask include wet chemical etching by use of HF and dry chemical etching by use of a gas mixture that gives rise to HF vapor during the etching process. The disadvantage of wet chemical etching is that it does not yield well con-

trolled, vertical sidewalls. The disadvantage of dry chemical etching as described above is that the SiO<sub>2</sub> is etched so quickly that one cannot ensure verticality of the sidewalls; in addition, the etching process causes the deposition of a carbonaceous polymeric residue that is thick enough to make it impossible to etch uniformly through the total thickness of the SiO<sub>2</sub>.

The essence of present RIE process is anisotropic etching of SiO<sub>2</sub> in CHF<sub>3</sub> with power kept low enough so as not to alter the shapes of the photoresist sidewalls and thereby to keep the SiO<sub>2</sub> sidewalls close to vertical. Unlike the mixtures of gases used previously, CHF<sub>3</sub> does not give rise to HF during this process. The recipe for this process is the following:

*First Etch* — CHF<sub>3</sub> flowing at a rate between 10 and 15 standard cubic centimeters per minute; power between 30 and 50 W; and pressure between 0 and 20 mtorr (between 0 and 2.7 Pa). The etch rate lies between 6 and 9 nm/s.

*Second Etch* — Same parameters as those of the first etch. The etching time should be

NASA's Jet Propulsion Laboratory,  
Pasadena, California

the time needed to complete the etch at the etch rate calculated from the result of the first etch.

By proceeding according to this recipe, one can minimize the buildup of the polymer and prevent both over-etching and undercutting. The angles between silicon substrates and sidewalls produced by this process range from 70° to 90°.

*This work was done by Tasha Turner and Chi Wu of Caltech for NASA's Jet Propulsion Laboratory. Further information is contained in a TSP [see page 1].*

*In accordance with Public Law 96-517, the contractor has elected to retain title to this invention. Inquiries concerning rights for its commercial use should be addressed to Intellectual Property group*

*JPL*

*Mail Stop 202-233*

*4800 Oak Grove Drive*

*Pasadena, CA 91109*

*(818) 354-2240*

*Refer to NPO-20776, volume and number of this NASA Tech Briefs issue, and the page number.*

## Annealing Would Improve β"—Alumina Solid Electrolyte

The objective is to prevent a sudden reduction of ionic conductivity.

A pre-operational annealing process is under investigation as a potential means of preventing a sudden reduction of ionic conductivity in a β"—alumina solid electrolyte (BASE) during use. On the basis of tests described below, the sudden reduction of ionic conductivity, followed by a slow recovery, has been found to occur during testing of the solid electrolyte and electrode components of an alkali metal thermal-to-electric converter (AMTEC) cell. This conductivity reduction may be observed quite infrequently; at lower operating temperatures, T < 1,073 K, it is not usually observed at all, while at T = 1,123–1,173 K, hundreds of hours may pass before conductivity reduction occurs. Only on tests running at higher operating temperatures for thousands of hours is this phenomenon regularly exhibited. The reduction of ionic conductivity would degrade the performance of an AMTEC cell. A pre-operational annealing process would help to sustain performance.

The tests involved, among others, maintaining BASE at a temperature between 1,050 and 1,170 K in the presence of low-pressure sodium vapor — an environment similar to that in a sodium AMTEC cell. It was observed that after a few tens to hundreds of hours in this environment, the ionic conductivity of BASE can fall suddenly to a lower value, and thereafter recover during several tens of hours. The decrease in ionic conductivity has been attributed to the formation of nanometer-thickness cracks, which would be high-resistance paths with respect to conduction of ions. The recovery of ionic conductivity has been attributed to closing of the cracks through sintering of β"—alumina grains.

The approach to annealing is based on the following line of reasoning: Some NaAlO<sub>2</sub> is incorporated into BASE during manufacture to facilitate sintering the ceramic to near 100-percent density. It is hypothesized that the cracks are initiated by the formation of voids, which, in turn,

NASA's Jet Propulsion Laboratory,  
Pasadena, California

form as a result of (1) a reaction in which NaAlO<sub>2</sub> is converted to Na<sub>2</sub>O and either β— or β"—alumina and (2) some or all of the Na<sub>2</sub>O escapes by vaporizing. If this hypothesis is correct, then it should be possible to perform a pre-operational anneal to (1) force the conversion of NaAlO<sub>2</sub> and the formation of voids and (2) sinter the BASE to close the voids. Sintering should strengthen the material and thereby help to prevent the formation of voids and microscopic cracks during operation. In addition, if the loss of NaAlO<sub>2</sub> during operation contributes to the loss of subsequently recoverable ionic conductivity, then the removal of NaAlO<sub>2</sub> in the pre-operational sintering process should help to stabilize the high-temperature ionic conductivity of BASE.

In an experiment, samples of β"—alumina ceramic containing ≈1 weight percent of NaAlO<sub>2</sub> were packed in a mixture of lithia-stabilized β"—alumina powder and sodium β—alumina powder in a loosely capped crucible, and annealed at a tem-

perature of 1,400 °C (1,673 K) in a vacuum for various times up to 100 hours. (The powder mixture was used to establish fixed low sodium  $\text{Na}_2\text{O}$  activity characteristic of the  $\beta/\beta''$  phase boundary. The  $\text{Na}_2\text{O}$  activity of this mixture is much lower than that above  $\text{NaAlO}_2$  and facilitates the loss of  $\text{Na}_2\text{O}$  from the  $\text{NaAlO}_2$  in the ceramic as well as sintering to close voids at grain boundaries.)

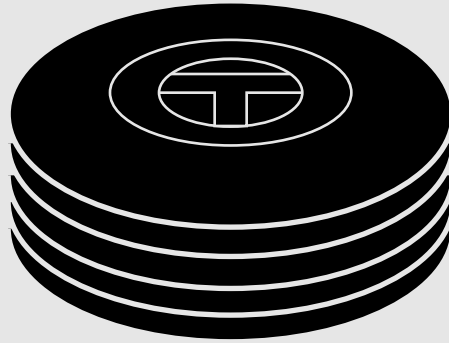
The  $\beta''$ -alumina samples were found to have lost an average of between 0.4 to 0.5 percent of mass during the 100-hour anneal; this amount of loss is consistent with the conversion of most of the  $\text{NaAlO}_2$  to  $\beta$ - or  $\beta''$ -alumina. (Complete conver-

sion would entail a mass loss of 0.5 percent.) Qualitative tests showed the mechanical characteristics of the samples to have been improved by the anneal.

At this time, high-temperature tests of limited duration have indicated the superiority of the treated BASE, but reproducible tests over thousands of hours are necessary to confirm that microcracking has been eliminated. The ionic conductivity of the treated BASE is also measured to be higher than untreated BASE at 1,073 K in low-pressure sodium vapor. Microcracking resulting in loss of conductivity was not observed with treated BASE in one high-temperature experiment, but this result

must be duplicated over very long testing times to be sure of the effect. Shorter annealing times (10 to 20 hours) were found to result in significantly less loss of mass; it may be necessary for the packed powder mixture to evolve some  $\text{Na}_2\text{O}$  before the  $\text{Na}_2\text{O}$  can leave the ceramic.

*This work was done by Roger Williams, Margie Homer, Margaret Ryan, Roger Cortez, Virgil Shields, and Adam Kisor of Caltech for NASA's Jet Propulsion Laboratory. Further information is contained in a TSP [see page 1].*  
NPO-20919



# Computer Programs

## **Electronic Systems**

- 29 Software for Remote Monitoring of Space-Station Payloads
- 29 SpaceWire Driver Software for Special DSPs

## **Mechanics**

- 29 Solution-Adaptive Program for Computing 2D/Axi Viscous Flow

## **Machinery**

- 29 Software for Preprocessing Data From Rocket-Engine Tests

## **Mathematics and Information Sciences**

- 30 Software for Automated Reading of STEP Files by I-DEAS™
- 30 Using a Portfolio of Algorithms for Planning and Scheduling
- 30 Software for Better Documentation of Other Software



# Computer Programs

## Electronic Systems

### Software for Remote Monitoring of Space-Station Payloads

Telescience Resource Kit (TReK) is a suite of application programs that enable geographically dispersed users to monitor scientific payloads aboard the International Space Station (ISS). TReK provides local ground support services that can simultaneously receive, process, record, playback, and display data from multiple sources. TReK also provides interfaces to use the remote services provided by the Payload Operations Integration Center which manages all ISS payloads. An application programming interface (API) allows for payload users to gain access to all data processed by TReK and allows payload-specific tools and programs to be built or integrated with TReK. Used in conjunction with other ISS-provided tools, TReK provides the ability to integrate payloads with the operational ground system early in the lifecycle. This reduces the potential for operational problems and provides "cradle-to-grave" end-to-end operations. TReK contains user guides and self-paced tutorials along with training applications to allow the user to become familiar with the system.

*This program was written by Michelle Schneider, Jeff Lippincott, Steve Chubb, Jimmy Whitaker, Robert Gillis, Donna Sellers, Chris Sims, and James Rice of Marshall Space Flight Center. Further information is contained in a TSP [see page 1].*  
MFS-31792

### SpaceWire Driver Software for Special DSPs

A computer program provides a high-level C-language interface to electronics circuitry that controls a SpaceWire interface in a system based on a space qualified version of the ADSP-21020 digital signal processor (DSP). SpaceWire is a spacecraft-oriented standard for packet-switching data-communication networks that comprise nodes connected through bidirectional digital serial links that utilize low-voltage differential signaling (LVDS). The software is tailored to the SMCS-332 application-specific integrated circuit (ASIC) (also available as the TSS901E), which provides three high-speed (150 Mbps) serial point-to-point links compliant with the proposed Institute of

Electrical and Electronics Engineers (IEEE) Standard 1355.2 and equivalent European Space Agency (ESA) Standard ECSS-E-50-12. In the specific application of this software, the SpaceWire ASIC was combined with the DSP processor, memory, and control logic in a Multi-Chip Module DSP (MCM-DSP). The software is a collection of low-level driver routines that provide a simple message-passing application programming interface (API) for software running on the DSP. Routines are provided for interrupt-driven access to the two styles of interface provided by the SMCS: (1) the "word at a time" conventional host interface (HOCI); and (2) a higher performance "dual port memory" style interface (COMI).

*This program was written by Douglas Clark, James Lux, Kouji Nishimoto, and Minh Lang of Caltech for NASA's Jet Propulsion Laboratory. Further information is contained in a TSP [see page 1].*

*This software is available for commercial licensing. Please contact Don Hart of the California Institute of Technology at (818) 393-3425. Refer to NPO-30389.*

## Mechanics

### Solution-Adaptive Program for Computing 2D/Axi Viscous Flow

A computer program solves the Navier-Stokes equations governing the flow of a viscous, compressible fluid in an axisymmetric or two-dimensional (2D) setting. To obtain solutions more accurate than those generated by prior such programs that utilize regular and/or fixed computational meshes, this program utilizes unstructured (that is, irregular triangular) computational meshes that are automatically adapted to solutions. The adaptation can refine to regions of high change in gradient or can be driven by a novel residual minimization technique. Starting from an initial mesh and a corresponding data structure, the adaptation of the mesh is controlled by use of minimization functional. Other improvements over prior such programs include the following: (1) Boundary conditions are imposed weakly; that is, following initial specification of solution values at boundary nodes, these values are relaxed in time by means of the same formulations as those used for interior nodes. (2) Eigenvalues are limited in order to suppress

expansion shocks. (3) An upwind fluctuation-splitting distribution scheme applied to inviscid flux requires fewer operations and produces less artificial dissipation than does a finite-volume scheme, leading to greater accuracy of solutions.

*This program was written by William A. Wood of Langley Research Center. Further information is contained in a TSP [see page 1].*  
LAR-16431

## Machinery

### Software for Preprocessing Data From Rocket-Engine Tests

Three computer programs have been written to preprocess digitized outputs of sensors during rocket-engine tests at Stennis Space Center (SSC). The programs apply exclusively to the SSC "E" test-stand complex and utilize the SSC file format. The programs are the following:

- Engineering Units Generator (EUGEN) converts sensor-output-measurement data to engineering units. The inputs to EUGEN are raw binary test-data files, which include the voltage data, a list identifying the data channels, and time codes. EUGEN effects conversion by use of a file that contains calibration coefficients for each channel.
- QUICKLOOK enables immediate viewing of a few selected channels of data, in contradistinction to viewing only after post-test processing (which can take 30 minutes to several hours depending on the number of channels and other test parameters) of data from all channels. QUICKLOOK converts the selected data into a form in which they can be plotted in engineering units by use of Winplot (a free graphing program written by Rick Paris).
- EUPLOT provides a quick means for looking at data files generated by EUGEN without the necessity of relying on the PV-WAVE based plotting software.

*This program was written by Chiu-Fu Cheng of Lockheed Martin Corp. for Stennis Space Center.*

*Inquiries concerning rights for the commercial use of this invention should be addressed to the Intellectual Property Manager, Stennis Space Center [see page 1]. Refer to SSC-00151/53/60.*

---

## Mathematics and Information Sciences

---

### Software for Automated Reading of STEP Files by I-DEAS™

A program called "readstep" enables the I-DEAS™ computer-aided-design (CAD) software to automatically read Standard for the Exchange of Product Model Data (STEP) files. (The STEP format is one of several used to transfer data between dissimilar CAD programs.) Prior to the development of "readstep," it was necessary to read STEP files into I-DEAS™ one at a time in a slow process that required repeated intervention by the user. In operation, "readstep" prompts the user for the location of the desired STEP files and the names of the I-DEAS™ project and model file, then generates an I-DEAS™ program file called "readstep.prg" and two Unix shell programs called "runner" and "controller." The program "runner" runs I-DEAS™ sessions that execute readstep.prg, while "controller" controls the execution of "runner" and edits readstep.prg if necessary. The user sets "runner" and "controller" into execution simultaneously, and then no further intervention by the user is required. When "runner" has finished, the user should see only parts from successfully read STEP files present in the model file. STEP files that could not be read successfully (e.g., because of format errors) should be regenerated before attempting to read them again.

*This program was written by John Pinedo of Lockheed Martin for Johnson Space Center. Further information is contained in a TSP [see page 1].*  
MSC-23192

### Using a Portfolio of Algorithms for Planning and Scheduling

The Automated Scheduling and Planning Environment (ASPEN) software system, aspects of which have been reported in several previous *NASA Tech Briefs* articles, includes a subsystem that utilizes a portfolio of heuristic algorithms that work synergistically to solve problems. The nature of the synergy of the specific algorithms is that their likelihoods of success are negatively correlated: that is, when a combination of them is used to solve a problem, the probability that at least one of them will succeed is greater than the sum of probabilities of success of the individual algorithms operating independently of each other. In ASPEN, the portfolio of algorithms is used in a planning process of the iterative repair type, in which conflicts are detected and addressed one at a time until either no conflicts exist or a user-defined time limit has been exceeded. At each choice point (e.g., selection of conflict; selection of method of resolution of conflict; or choice of move, addition, or deletion) ASPEN makes a stochastic choice of a combination of algorithms from the portfolio. This approach makes it possible for the search to escape from looping and from solutions that are locally but not globally optimum.

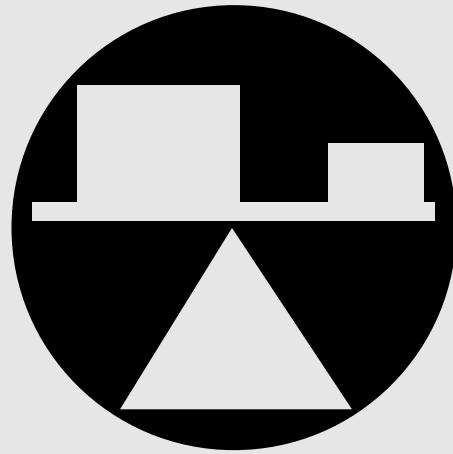
*This program was written by Robert Sherwood, Russell Knight, Gregg Rabideau, Steve Chien, Daniel Tran, and Barbara Engelhardt of Caltech for NASA's Jet Propulsion Laboratory. Further information is contained in a TSP [see page 1].*

*This software is available for commercial licensing. Please contact Don Hart of the California Institute of Technology at (818) 393-3425. Refer to NPO-30379.*

### Software for Better Documentation of Other Software

The Literate Programming Extraction Engine is a Practical Extraction and Reporting Language- (PERL-)based computer program that facilitates and simplifies the implementation of a concept of self-documented literate programming in a fashion tailored to the typical needs of scientists. The advantage for the programmer is that documentation and source code are written side-by-side in the same file, reducing the likelihood that the documentation will be inconsistent with the code and improving the verification that the code performs its intended functions. The advantage for the user is the knowledge that the documentation matches the software because they come from the same file. This program unifies the documentation process for a variety of programming languages, including C, C++, and several versions of FORTRAN. This program can process the documentation in any markup language, and incorporates the LaTeX typesetting software. The program includes sample Makefile scripts for automating both the code-compilation (when appropriate) and documentation-generation processes into a single command-line statement. Also included are macro instructions for the Emacs display-editor software, making it easy for a programmer to toggle between editing in a code or a documentation mode.

*This program was written by William A. Wood and William L. Kleb of Langley Research Center. Further information is contained in a TSP [see page 1].*  
LAR-16438



# Mechanics

## Hardware, Techniques, and Processes

33      Docking Fixture and Mechanism for a Protective Suit



## Docking Fixture and Mechanism for a Protective Suit

One can transfer safely and quickly between the suit and a sealed vehicle.

Ames Research Center,  
Moffett Field, California

A suitlock assembly that comprises a docking fixture and mechanism has been invented to facilitate and accelerate donning and doffing of a sealed protective suit and/or to enable ingress and egress between the protective suit and a sealed vessel. The sealed protective suit could be a space suit, in which case the sealed vessel could be a spacecraft. Alternatively, the sealed suit could be an environmental protective suit of a type worn on Earth during cleanup of a hazardous-material site, in which case the sealed vessel could be a vehicle equipped to maintain a safe interior environment for workers in transit to and from the site. Figure 1 depicts a typical situation in which several crewmembers are working inside such a vehicle, one is working outside in a protective suit, and one is donning or doffing a protective suit while holding onto an overhead bar for support.

The suitlock assembly surrounds a large opening in the back of the suit and can be attached to or detached from a containment assembly or hatch on the vehicle. A person enters or leaves the suit through the opening surrounded by the suitlock assembly. Once the person is inside the suit, the

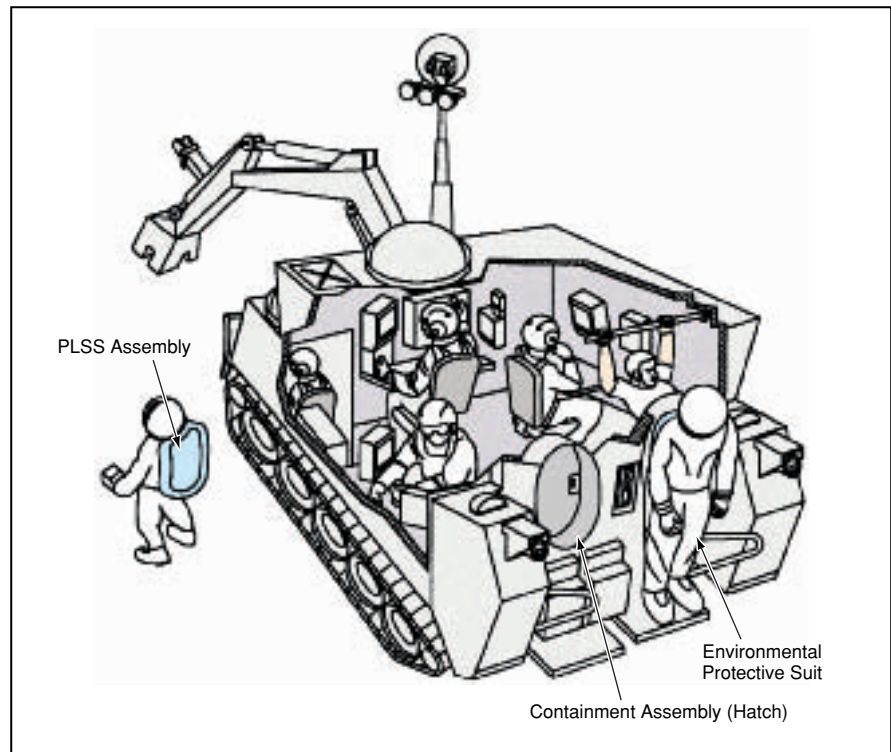


Figure 1. A Sealed Vehicle Includes Hatches that enable workers to transfer between the interior of the vehicle and the interiors of protective suits that must be worn outside the vehicle.

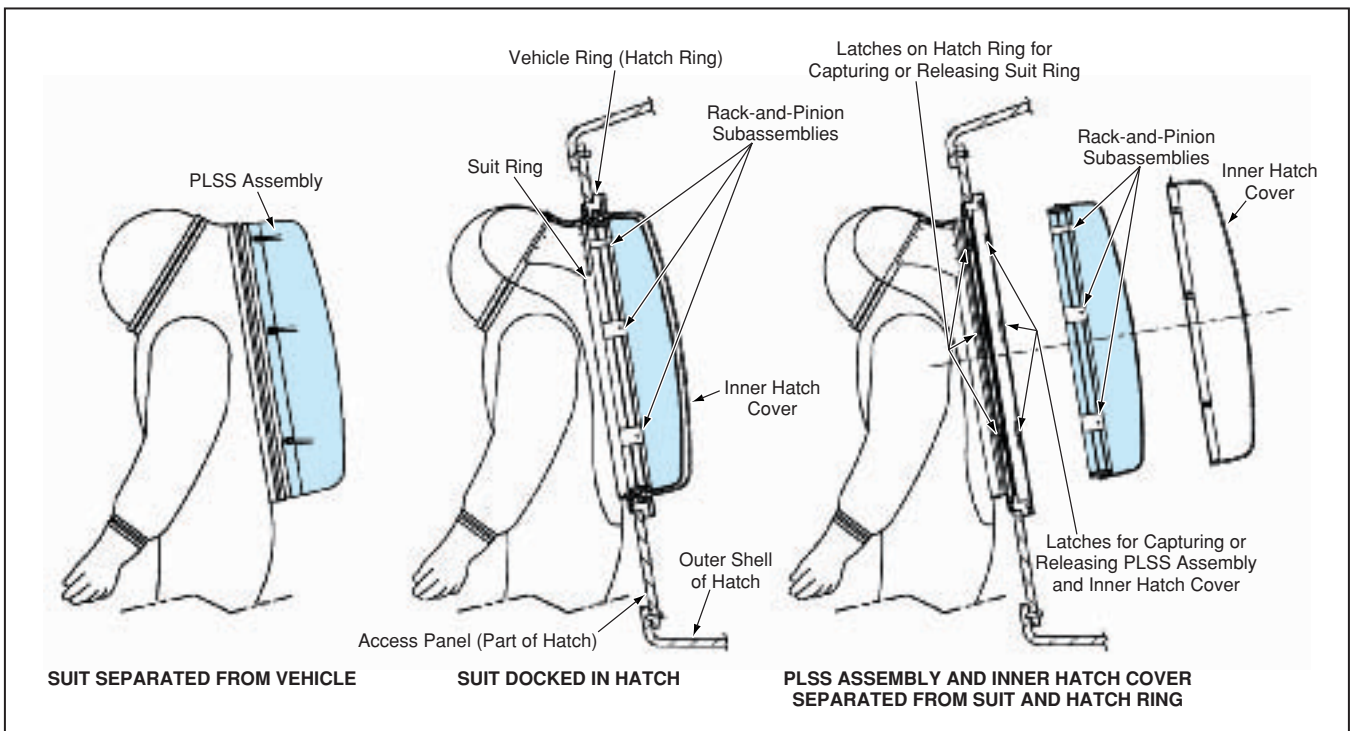


Figure 2. The **Suitlock Assembly, PLSS Assembly, and Hatch** are all designed to function cooperatively for relatively rapid coupling and uncoupling of the sealed suit and the sealed vehicle, coupling and uncoupling of the PLSS assembly and the suit, and transfer of the PLSS assembly and the wearer through the hatch at the appropriate phases of operation.

suitlock assembly serves as a means for attaching or detaching a portable life-support system (PLSS) assembly, which is sealed to the suitlock assembly and provides breathing air and cooling when the wearer is sealed in the suit.

In preparation for leaving the suit and entering the vehicle, the wearer maneuvers backward, inserting the PLSS assembly into a recess in the hatch. The wearer then pushes backward until a suit ring and elastomeric seals on the suitlock assembly mate with sealing surfaces on a vehicle ring on the hatch and spring-loaded latches capture the suitlock assembly in the hatch. The seals protect the interiors of both the suit and the hatch against the external envi-

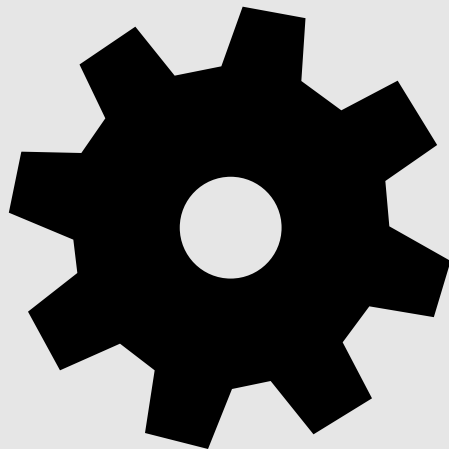
ronment. The interior of the hatch can then be purged to remove any contamination brought in from the outside. Once the purge is complete, it is safe to open the hatch to the interior of the vehicle.

The wearer turns a handle (not shown in the figures) at the lower right corner of the suitlock assembly to actuate a cable linkage that, in turn, actuates latches and rack-and-pinion subassemblies at several positions around the periphery of the opening. The overall effect of this action is to detach the PLSS assembly from the suit and the inner hatch cover from the hatch ring and to transfer the PLSS assembly into the hatch. The inner hatch cover and the PLSS assembly can then be taken into

the interior of the vehicle to make room for the wearer to leave the suit and enter the vehicle. The foregoing sequence of operations is reversed for a wearer donning the suit and leaving the vehicle.

*This work was done by Philip Culbertson, Jr., of **Ames Research Center**. Further information is contained in a TSP [see page 1].*

*This invention has been patented by NASA (U.S. Patent No. 5,697,108). Inquiries concerning nonexclusive or exclusive license for its commercial development should be addressed to the Patent Counsel, Ames Research Center, (650) 604-5104. Refer to ARC-14102.*



# Machinery

## Hardware, Techniques, and Processes

- 37 Compliant Gripper for a Robotic Manipulator
- 37 Hybrid Aerial/Rover Vehicle



## Compliant Gripper for a Robotic Manipulator

Diverse small objects can be manipulated without force-feedback control.

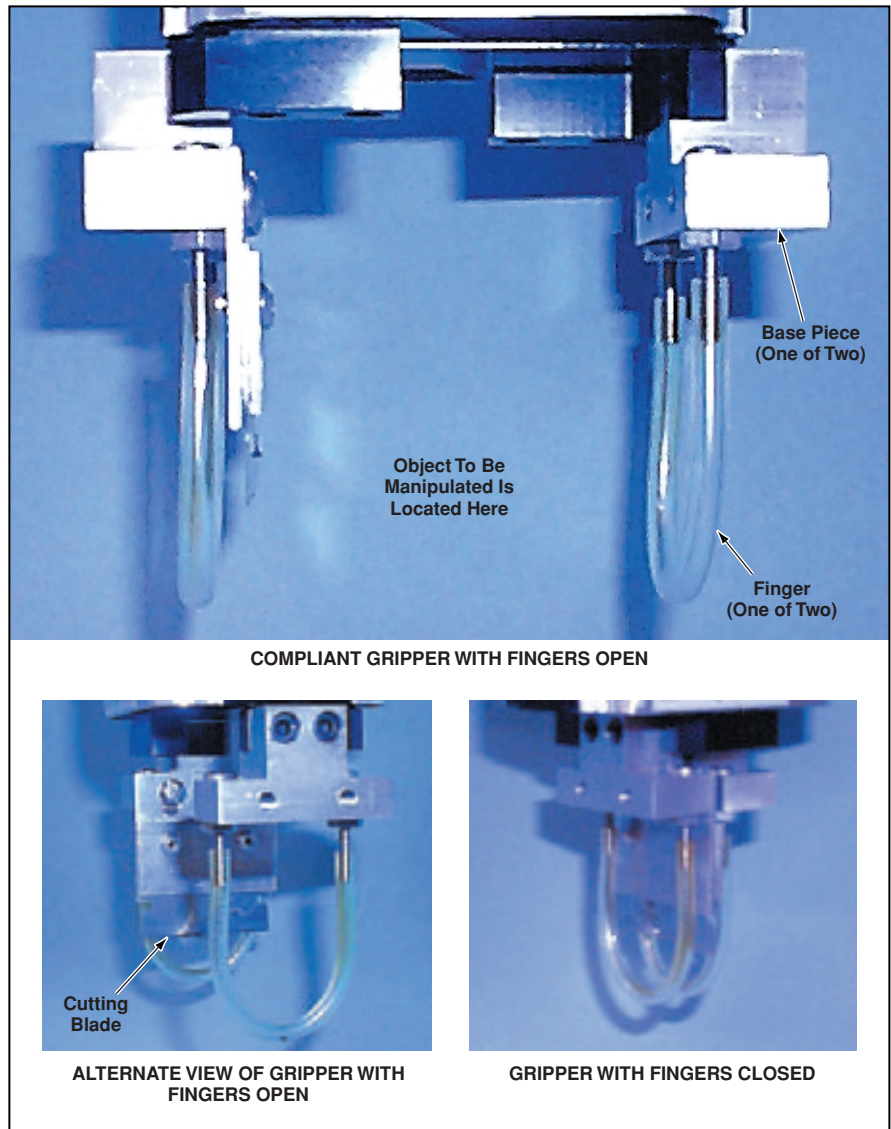
NASA's Jet Propulsion Laboratory,  
Pasadena, California

The figure depicts a prototype of a robotic-manipulator gripping device that includes two passive compliant fingers, suitable for picking up and manipulating objects that have irregular shapes and/or that are, themselves, compliant. The main advantage offered by this device over other robotic-manipulator gripping devices is simplicity: Because of the compliance of the fingers, force-feedback control of the fingers is not necessary for gripping objects of a variety of sizes, shapes, textures, and degrees of compliance. Examples of objects that can be manipulated include small stones, articles of clothing, and parts of plants.

The device includes two base pieces that translate relative to each other to effect opening and closing of the compliant gripping fingers. Each finger is made of a piece of elastomeric tubing bent into a U shape and attached at both ends to one of the base pieces. This arrangement of the finger provides compliance, both in orientation and in translation along all three spatial dimensions.

Because the specific application for which this device was designed involves picking up and cutting plant shoots for propagation of the plants, the device includes a cutting blade attached to one of the base pieces. By positioning the device to hold an object, then closing the fingers to grip the object, then driving the base pieces downward toward the object, one can cause the blade to cut the object into two pieces. Because, prior to cutting, the fingers are both holding the object and in contact with the surface on which the object is resting, it is possible to move the base pieces sideways simultaneously to center the blade while keeping the object immobile.

The prototype gripper has been shown to be capable of picking up a small object. There is a need to refine the design of the gripper; in particular, there is a need to incorporate a sensor that would measure the position of an object relative to that of



This **Gripping Device** can manipulate and cut a plant shoot or other small object.

the gripper. Other aspects of the design expected to be refined in continuing development include the general problem of gripping, the method of actuation for closing the fingers, the shape of the fingers, fixturing, and cutting.

*This work was done by Raymond*

*Cipra, NASA Summer Faculty Fellow from Purdue University, and Hari Das of Caltech for NASA's Jet Propulsion Laboratory. Further information is contained in a TSP [see page 1]. NPO-21104*

## Hybrid Aerial/Rover Vehicle

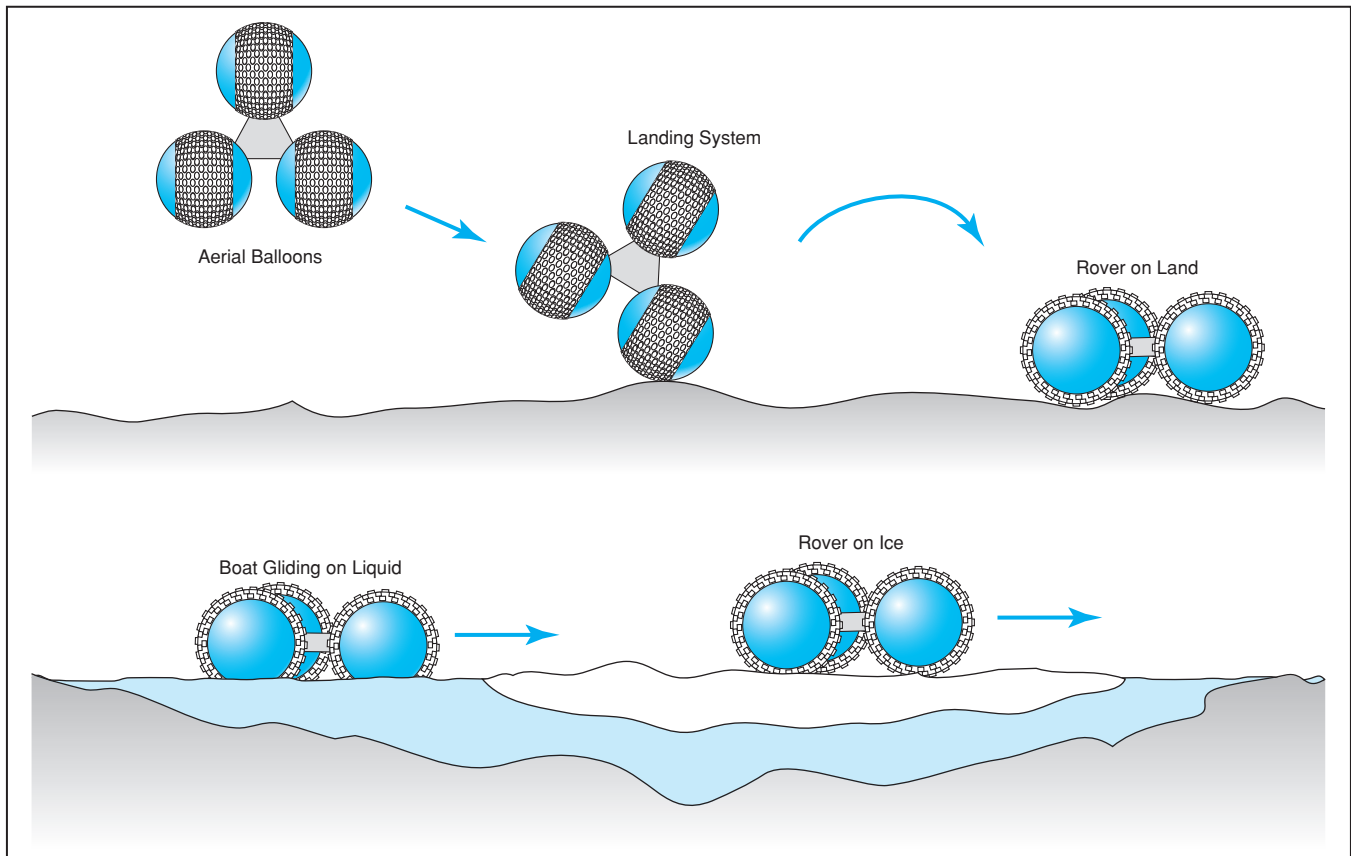
This robotic vehicle would combine features of balloons and "beach-ball" rovers.

NASA's Jet Propulsion Laboratory,  
Pasadena, California

A proposed instrumented robotic vehicle called an "aerover" would fly, roll along the ground, and/or float on bodies of liquid, as

needed. The aerover would combine features of an aerobot (a robotic lighter-than-air balloon) and a wheeled robot of the "rover"

class. An aerover would also look very much like a variant of the "beach-ball" rovers described in "Lightweight 'Beach-



The **Aerover** would fly, roll on solid surfaces, and/or glide on liquid to acquire scientific data at selected locations along the way.

Ball' Robotic Vehicles" (NPO-20283), *NASA Tech Briefs*, Vol. 22, No. 7 (July 1998), page 74. Although the aerover was conceived for use in scientific exploration of Titan (the largest moon of the planet Saturn), the aerover concept could readily be adapted to similar uses on Earth.

The aerover would include three thick-walled balloons (see figure), each about 2 m in diameter. Initially, the balloons would be inflated with helium to provide lift for flight. Later the balloons would also serve as cushions for landing, as soft tires for rolling over the ground, as flotation bags for traversing bodies of liquid, and as thermal barriers to protect instrument payloads against extreme cold on the ground.

Following initial inflation, the aerover would be set free to drift at a controlled altitude, gathering images of terrain. Altitude

control could be effected by (1) heating and/or inflation from a supply tank for ascent and (2) venting helium and/or turning off the heater for descent. From time to time, helium would be vented to make the aerover descend to collect ground samples by use of tethered coring modules or a landing snake. Thereafter, the aerover would make several ascents and descents to acquire additional images and samples.

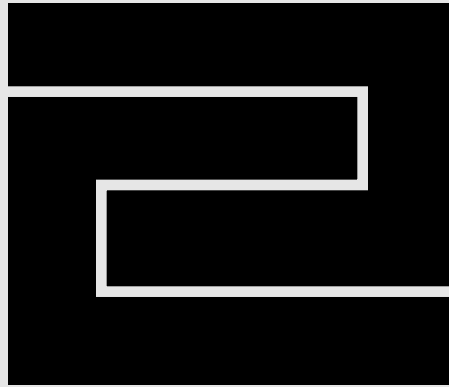
Eventually, the helium supply would approach depletion; helium would then be vented gradually to effect a final descent. The residual helium in the balloons would provide cushion for a soft landing. Thereafter, the aerover would remain permanently on the surface.

Once the aerover was on the surface, the residual helium in the balloons would be replaced with ambient air. The aerover

would then roll along the ground and/or traverse liquid to travel to designated sites, where it would collect highly localized images and samples.

The three-balloon design concept is a fail-safe one. The aerover would be designed so that two functional balloons would provide sufficient lift for ascent. Three balloons would afford redundancy to protect against a failure of one of the balloons. If all three balloons were intact and functioning as intended, then the aerover would have a capability for initial overinflation.

*This work was done by Aaron Bachelder of Caltech for NASA's Jet Propulsion Laboratory. Further information is contained in a TSP [see page 1].*  
NPO-20609



# Fabrication Technology

## Hardware, Techniques, and Processes

- 41 Tool For Friction Stir Tack Welding of Aluminum Alloys
- 41 Improving Plating by Use of Intense Acoustic Beams



## Tool For Friction Stir Tack Welding of Aluminum Alloys

The same setup can be used for tack welding and full friction stir welding.

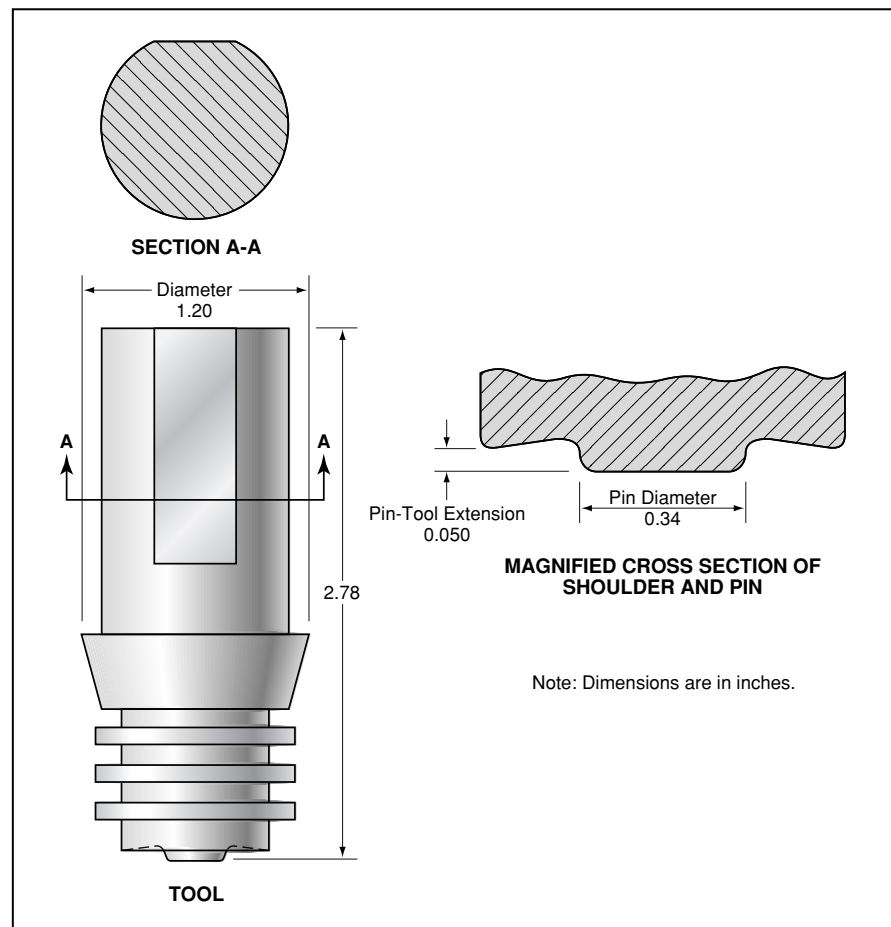
Marshall Space Flight Center,  
Alabama

A small friction-stir-welding tool has been developed for use in tack welding of aluminum-alloy workpieces. It is necessary to tack-weld the workpieces in order to hold them together during friction stir welding because (1) in operation, a full-size friction-stir-welding tool exerts a large force that tends to separate the workpieces and (2) clamping the workpieces is not sufficient to resist this force.

It is possible to tack the pieces together by gas tungsten arc welding, but the process can be awkward and time-consuming and can cause sufficient damage to necessitate rework. Friction stir tack welding does not entail these disadvantages. In addition, friction stir tack welding can be accomplished by use of the same automated equipment (except for the welding tool) used in subsequent full friction stir welding.

The tool for friction stir tack welding (see figure) resembles the tool for full friction stir welding, but has a narrower shoulder and a shorter pin. The shorter pin generates a smaller workpiece-separating force so that clamping suffices to keep the workpieces together. This tool produces a continuous or intermittent partial-penetration tack weld. The tack weld is subsequently consumed by action of the larger tool used in full friction stir welding tool.

*This work was done by Gerald W. Bjorkman, Johnny W. Dingle, and Zachary Loftus of Lockheed Martin Corp. for Marshall Space Flight Center. Further information is contained in a TSP [see page 1].*  
MFS-31392



This **Friction-Stir-Welding Tool** is designed specifically for tack welding of 0.32-in. (8.1-mm)-thick pieces of aluminum-lithium alloy 2195. Different values of pin-tool extension and shoulder diameter might be needed for optimum tack welding of different alloys or different thicknesses.

## Improving Plating by Use of Intense Acoustic Beams

This method affords enhanced capabilities for maskless plating and process control.

John H. Glenn Research Center,  
Cleveland, Ohio

An improved method of selective plating of metals and possibly other materials involves the use of directed high-intensity acoustic beams. The beams, typically in the ultrasonic frequency range, can be generated by fixed-focus transducers (see figure) or by phased arrays of transducers excited, variously, by continuous waves, tone bursts, or single pulses. The nonlinear effects produced by these beams are used to alter plating processes in ways that are advantageous.

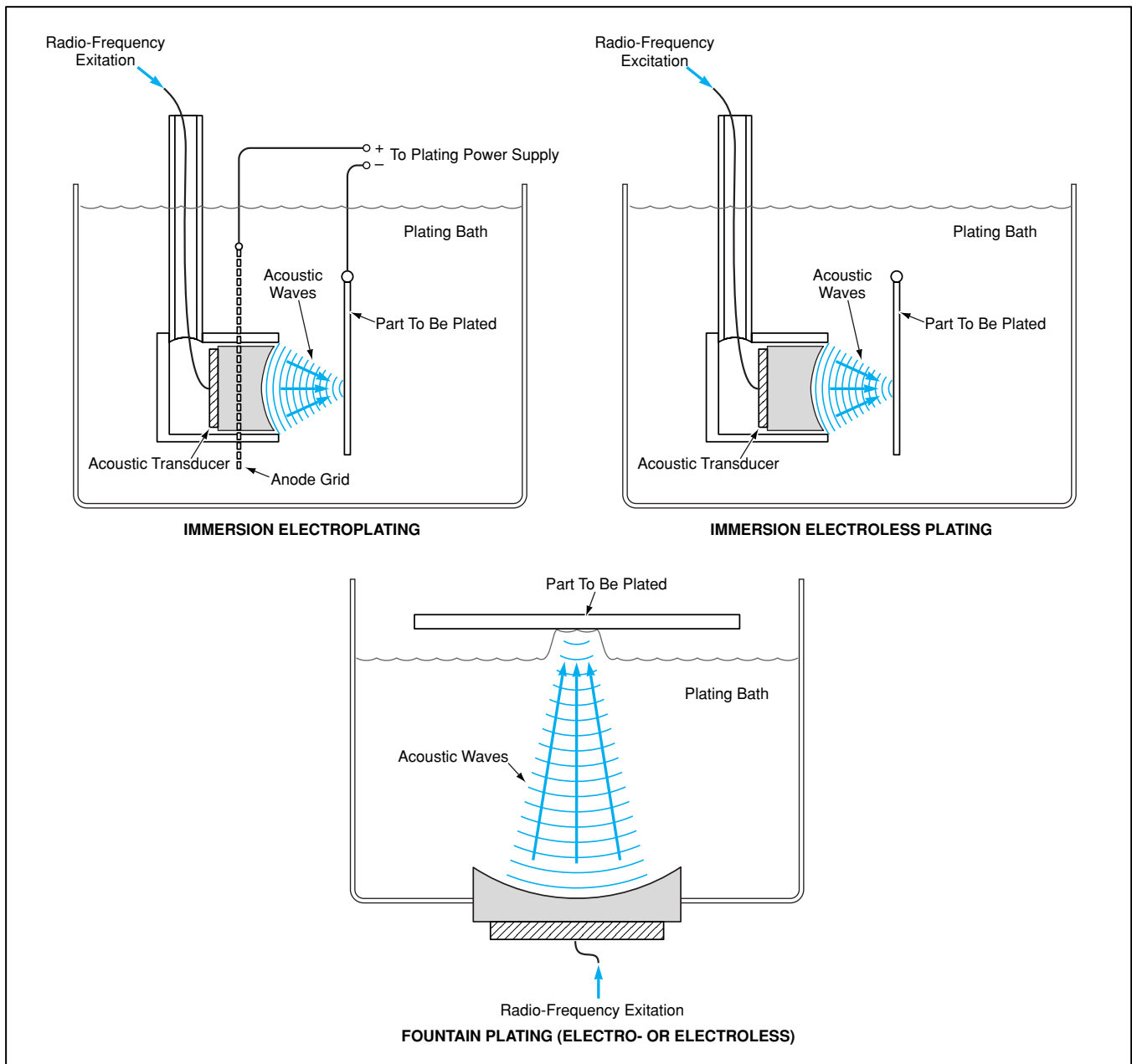
One of the nonlinear effects is acoustic streaming, which can contribute to selective plating of an object immersed in a plat-

ing solution by providing fresh plating solution to the portion of the object at or near the focus of a beam. The combination of acoustic streaming and acoustic-radiation pressure is effective in removing debris and bubbles, which, if allowed to remain, can contaminate the plating material and/or inhibit the plating process. Acoustic streaming can also be used to reduce concentrations and gradients of concentrations of gases (especially hydrogen) in order to prevent the formation of bubbles. Acoustic streaming can be utilized further to counteract effects of localized electric fields and of gradients of concentration of

the plating solution that can give rise to undesired components of spatial nonuniformity in the plating process.

Another nonlinear effect is heating of the plating solution in the focal region. The local increase in temperature causes a local increase in the rates of chemical reactions and thus in the rate of deposition of plating material.

As an alternative to the immersion form of selective plating, acoustic streaming can be utilized to create a fountain of plating solution, which strikes a selected small area of a part suspended over a pool of plating solution. Plating occurs only on the



**Focused Acoustic Beams** can be used to enhance electroplating or electroless plating in a variety of different configurations.

area in contact with the plating solution. Whether the immersion or the fountain version of the method is used, the spatial selectivity afforded by the method reduces the need for masking materials, masking processes, and masking devices.

The maskless-plating capability afforded by this method is most applicable to plating applications in which small amounts of excess plating in the areas outside the acoustic-beam focal regions are tolerated or in which plating processes can be reversed to remove this excess plating. An example of such an application

is that of a circuit board coated over its entire surface with a thin layer of gold to increase its resistance to corrosion and enhance its solderability. Typically, there is a need for thicker gold plating in specific locations on such a circuit board — especially at connector contact areas or push-button contact points, where there is a need to maintain reliable electrical contacts in the presence of physical wear. The present method makes it possible to plate metal onto the board with spatially varying thickness in a single operation, without masking.

*This work was done by Richard C. Oeffering of **Glenn Research Center** and Charles Denofrio of Alchemitron Corp. Further information is contained in a TSP [see page 1].*

*Inquiries concerning rights for the commercial use of this invention should be addressed to NASA Glenn Research Center, Commercial Technology Office, Attn: Steve Fedor, Mail Stop 4-8, 21000 Brookpark Road, Cleveland, Ohio 44135. Refer to LEW-17041.*



# Mathematics and Information Sciences

## Hardware, Techniques, and Processes

- 45 Efficient Processing of Data for Locating Lightning Strikes
- 46 P-Code-Enhanced Encryption-Mode Processing of GPS Signals
- 47 Integrated Formulation of Beacon-Based Exception Analysis for  
Multimissions
- 48 Determining Direction of Arrival at a Y-Shaped Antenna Array
- 49 Self-Supervised Dynamical Systems



# Efficient Processing of Data for Locating Lightning Strikes

Time differences can be computed efficiently to subnanosecond resolution.

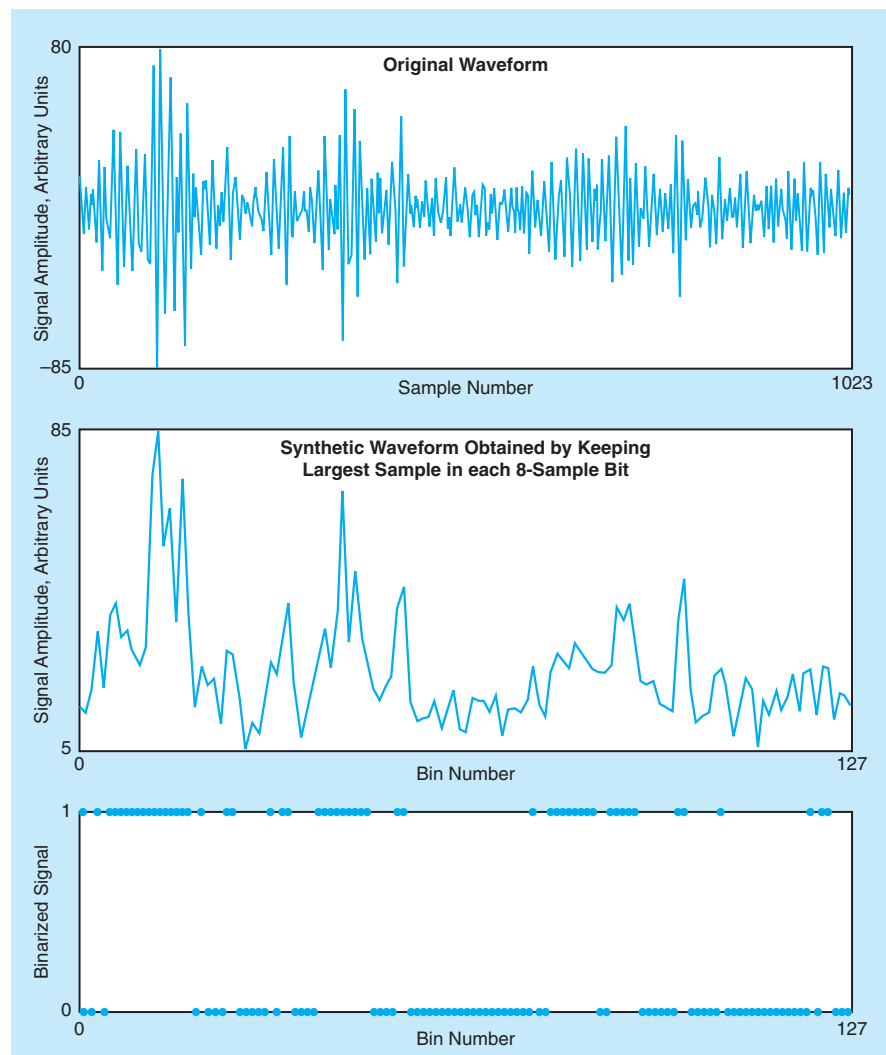
*John F. Kennedy Space Center,  
Florida*

Two algorithms have been devised to increase the efficiency of processing of data in lightning detection and ranging (LDAR) systems so as to enable the accurate location of lightning strikes in real time. In LDAR, the location of a lightning strike is calculated by solving equations for the differences among the times of arrival (DTOAs) of the lightning signals at multiple antennas as functions of the locations of the antennas and the speed of light. The most difficult part of the problem is computing the DTOAs from digitized versions of the signals received by the various antennas. One way (a time-domain approach) to determine the DTOAs is to compute cross-correlations among variously differentially delayed replicas of the digitized signals and to select, as the DTOAs, those differential delays that yield the maximum correlations. Another way (a frequency-domain approach) to determine the DTOAs involves the computation of cross-correlations among Fourier transforms of variously differentially phased replicas of the digitized signals, along with utilization of the relationship among phase difference, time delay, and frequency.

One of the two algorithms is a computationally efficient implementation of the time-domain approach. This algorithm is intended specifically for use in an LDAR system in which the antennas are located at spatial intervals of about 100 m, the receiver at each antenna digitizes the signal at a rate of 500 megasamples per second, the signal is processed in successive 1,024-sample (2.048- $\mu$ s) time windows for the purpose of correlating it with 128-sample windows from the other antennas, and it is desired to compute 30,000 locations per second.

This algorithm includes the following steps:

1. Every 1,024-sample record is divided into 128 bins, each containing 8 consecutive samples.
2. The largest sample value within each bin is kept, and the other 7 samples are discarded, thus leaving 128 data points.
3. The average of the 128 remaining sample values is calculated.
4. Every sample value equal to or larger than the average is assigned a 1 and every sample value below the average is assigned a 0 (see figure).
5. The 128 resulting binary data are then stored as 16 bytes of 8 bits each.



**A Waveform Originally Sampled at 1,024 Points** is subsampled at peaks within 128 bins, then binarized.

6. Once the data from each antenna have been processed as described above, a bit-to-bit cross-correlation is performed between a 16-byte record from one channel and a 4-byte record from another channel. Because this is a bit-to-bit operation, it can easily be performed in real time by use of a field-programmable gate array (FPGA) integrated circuit. The result of operation 6 is a set of rough estimates of the cross-correlations.
7. Using the rough estimates as guides, finer estimates are obtained by calculating cross-correlations on the original digitized (but the binarized) sample data over a range from 16 samples before to 16 samples after the differential delay found from the rough estimate.

Whereas the computing power needed to generate the fine estimates by processing all of the original sample data is 3.44 gigaflops, the computing power needed to arrive at the fine estimates by way of this algorithm is only 122 megaflops. This amount of computing power lies within the range of available digital signal-processing integrated-circuit chips.

The time-domain algorithm described above cannot determine time differences to less than the 2-ns sample period. The other algorithm implements a frequency-domain approach to obtain higher temporal resolution. The frequency-domain algorithm includes the following steps:

1. The algorithm described above is used to obtain estimates of DTOAs to within

- a resolution of 2 ns.
- Waveforms from the various antennas are paired and temporally aligned with each other according to the 2-ns-resolution DTOAs.
  - The waveforms are windowed to prevent the introduction of extraneous frequency components.
  - A fast Fourier transform (FFT) is computed for each waveform. Because the receivers at the antennas operate in the

- 30-to-38- and 110-to-200-MHz frequency bands only, it is possible to limit the FFTs to these frequency bands, without loss of signal information, to reduce the computational burden.
- Within each pair, the phase difference between the FFTs of the two signals is computed for each frequency. For each pair, the time difference that corresponds to the phase difference for each frequency is calculated, then an effective delay

for the pair is calculated as a weighted sum of the time differences in all of the FFT frequency intervals.

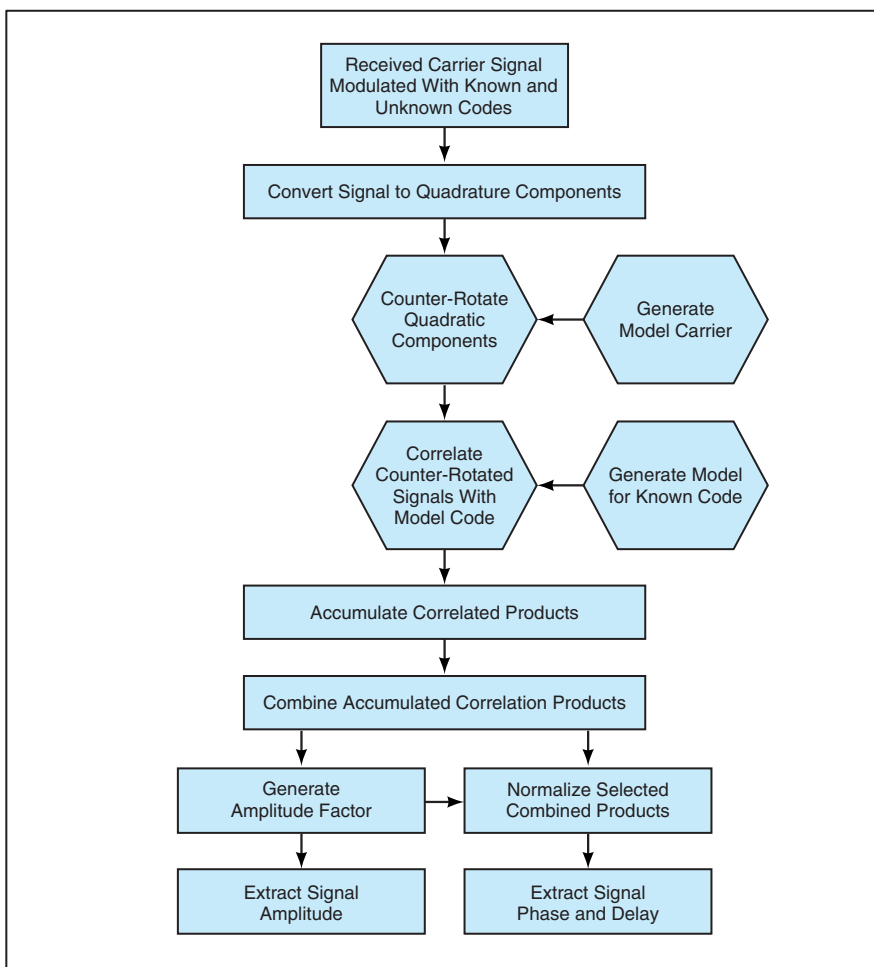
- For each pair, the effective delay is added to the starting 2-ns-resolution DTOA to obtain a more precise DTOA.

*This work was done by Pedro J. Medelius and Stan Starr of Dynacs, Inc., for Kennedy Space Center. Further information is contained in a TSP [see page 1].*  
KSC-12064/71

## P-Code-Enhanced Encryption-Mode Processing of GPS Signals

This is an improved method of processing without knowledge of the encryption code.

NASA's Jet Propulsion Laboratory,  
Pasadena, California



**P-Code-Enhanced Encryption-Mode Processing** of GPS signals according to the present invention involves this sequence of steps.

A method of processing signals in a Global Positioning System (GPS) receiver has been invented to enable the receiver to recover some of the information that is otherwise lost when GPS signals are encrypted at the transmitters. The need for this method arises because, at the option of the military, precision GPS code (P-code) is sometimes

encrypted by a secret binary code, denoted the A code. Authorized users can recover the full signal with knowledge of the A-code. However, even in the absence of knowledge of the A-code, one can track the encrypted signal by use of an estimate of the A-code. The present invention is a method of making and using such an estimate. In comparison

with prior such methods, this method makes it possible to recover more of the lost information and obtain greater accuracy.

The limitation on space available for this article precludes a description of the prior methods. However, a description of pertinent generally applicable aspects of GPS signals and signal processing is presented in the next three paragraphs because it is prerequisite to a meaningful summary of the present method.

Each GPS satellite transmits two L-band signals, denoted L1 (at a carrier frequency of 1.57542 GHz) and L2 (at a carrier frequency of 1.2276 GHz). The L1 carrier is phase-modulated with two binary pseudorandom-noise codes that contain GPS information: (1) the coarse-acquisition (C/A) code, characterized by a chip rate of 1.023 MHz and (2) the precise (P) code, characterized by a chip rate of 10.23 MHz and modulated in quadrature with the C/A code. The L2 carrier is modulated with the P code only. The signals from different satellites are distinguishable from each other because each satellite transmits a unique C/A and a unique P code. Although the limitation on space also precludes a detailed description of the C/A and P codes, it can be said here that names of these codes convey an approximate idea of the roles played by these codes and of the relationship between them. The C/A and P codes of all the satellites are further modulated with a common binary code that conveys information about the satellites, their orbits, their clock offsets, and their operational statuses.

The basic principle of GPS receiver signal processing is to determine the time and the position of the GPS receiver from times of arrival of signals transmitted from several different GPS satellites. This basic principle is implemented, in practice, by use of correlations between (1) the received GPS signals and (2) model signals in the receiver

constructed from model carriers modulated by model C/A, and P (and, when applicable, A) codes.

Processing is said to be done in a code mode when the receiver “knows” the code in question. Because the C/A code is not encrypted, C/A modulation is usually processed in the code mode, using the published C/A code. Processing is said to be done in an encryption mode when the receiver does not “know” the code in question. More specifically, processing is said to be done in an encryption mode when the receiver does not “know” the A code with which the P code is modulated. Hence, the present invention is characterized as a method of encryption-mode processing.

The figure is a block diagram of signal processing according to the invention. The received GPS signal is down-converted from radio frequency (RF) to baseband to obtain two pairs of quadrature components — one pair for L1, the other for L2. Unlike in some prior methods, there is no cross-processing of signals between the L1 and L2 P channels. Instead, each of the two quadrature components obtained from each RF signal, independently of the other components, is counterrotated with its

respective model phase, correlated with its respective model P code, and then successively summed and dumped over pre-sum intervals substantially coincident with chips of the respective encryption code. In the encryption mode, the effect of the unknown A-code sign flips is reduced, for each quadrature component of each RF signal, by combining selected pre-sums. The resulting combined pre-sums are then summed and dumped over longer intervals and further processed to extract the amplitude, phase, and delay for each RF signal. The precision of the resulting phase and delay values is approximately four times better than that obtained from conventional cross-correlation of the L1 and L2 P signals.

In comparison with prior encryption-mode receivers, a receiver according to this invention offers greater signal-to-noise ratios for the L1 and L2 P signals, and greater precision in the phases and delays of these signals. Unlike the prior receivers, this receiver offers the capability for separate and independent tracking of the L1 and L2 P signals to eliminate fading crossover, separate and independent measurement of the L1 and L2 P amplitudes, the option of dual-band measurements without a separate L1 P channel,

removal of a half-cycle ambiguity in the L2 P phase, and the option of operation in either the code mode or the encryption mode with maximum commonality of hardware and software between modes. Finally, this processing method would still work even if the L1 and L2 P codes were to be encrypted with different A codes.

*This work was done by Lawrence Young, Thomas Meehan, and Jess B. Thomas of Caltech for NASA's Jet Propulsion Laboratory. Further information is contained in a TSP [see page 1].*

*In accordance with Public Law 96-517, the contractor has elected to retain title to this invention. Inquiries concerning rights for its commercial use should be addressed to Intellectual Assets Office*

*JPL*

*Mail Stop 202-233*

*4800 Oak Grove Drive*

*Pasadena, CA 91109*

*(818) 354-2240*

*E-mail: ipgroup@jpl.nasa.gov*

*Refer to NPO-30367, volume and number of this NASA Tech Briefs issue, and the page number.*

## Integrated Formulation of Beacon-Based Exception Analysis for Multimissions

BEAM has become a broadly applicable, highly capable means of automated diagnosis.

Further work on beacon-based exception analysis for multimissions (BEAM), a method of real-time, automated diagnosis of a complex electromechanical systems, has greatly expanded its capability and suitability of application. This expanded formulation, which fully integrates physical models and symbolic analysis, is described architecturally in the figure.

In a typical application, BEAM takes the form of an embedded software suite executing onboard the system under study, though many off-board data analysis engines have been constructed as well. The BEAM software performs real-time fusion and analysis of all system observables. BEAM is intended to reduce the burden of diagnostic data collection and analysis currently performed by both human operators and computers. In the case of a spacecraft or aircraft, BEAM enables onboard identification and characterization of most anomalous conditions, thereby making telemetry of larger quantities of sensor information to ground stations unnecessary. Previously BEAM has been described in several prior *NASA Tech Briefs* articles: “Reusable Software for

Autonomous Diagnosis of Complex Systems” (NPO-20803) Vol. 26, No. 3 (March 2002), page 33; “Beacon-Based Exception Analysis for Multimissions” (NPO-20827), Vol. 26, No. 9 (September 2002), page 32; and “Wavelet-Based Real-Time Diagnosis of Complex Systems” (NPO-20830), Vol. 27, No. 1 (January 2003), page 67.

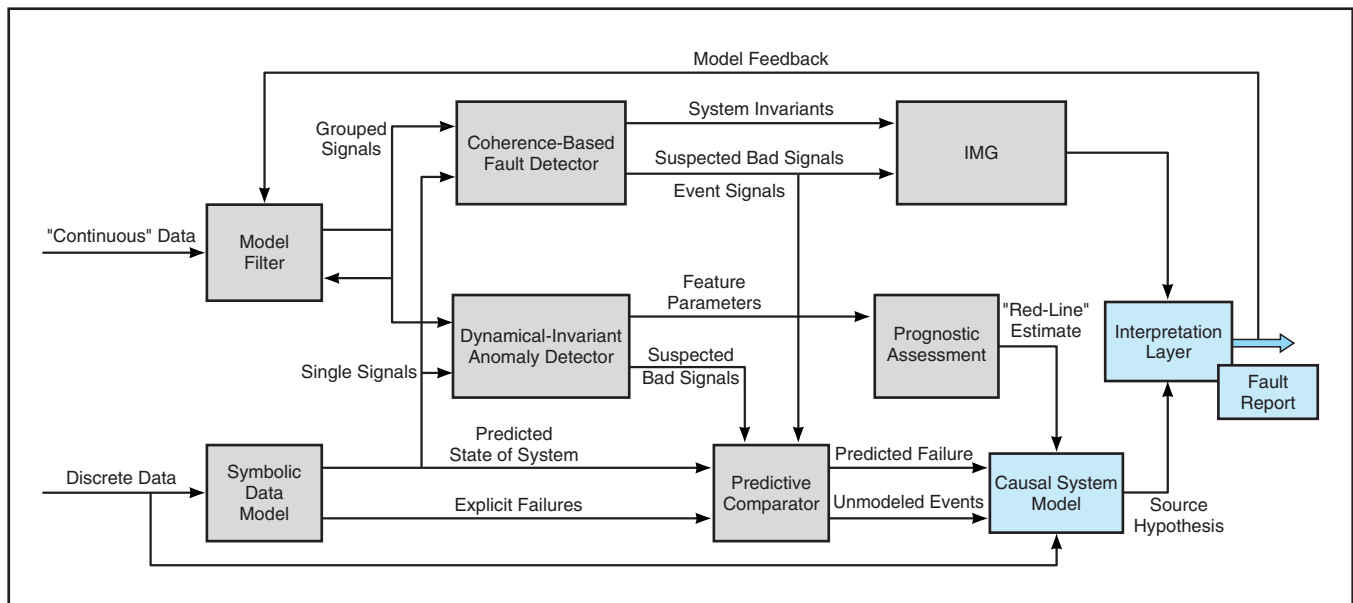
The new formulation of BEAM expands upon previous advanced techniques for analysis of signal data, utilizing mathematical modeling of the system physics, and expert-system reasoning. These components are integrated seamlessly, making possible analysis of varied information about the monitored system, including time-correlated signal performance, state information, software execution, operator command execution, and convergence to state and physical models. BEAM software is highly adaptable and can be implemented at relatively low cost in terms of processor power and training, and does not require special sensors. Unlike some prior methods of automated diagnosis, BEAM affords traceability of its conclusions, which allows system experts to

*NASA's Jet Propulsion Laboratory,  
Pasadena, California*

completely reconstruct its decision path for greater operator confidence or to aid analysis of novel conditions. Principal among BEAM's strengths is its excellent performance in detection and classification of such novelty, meaning faults of previously unknown — and untrainable — type.

In the BEAM architecture, discrete sensor information, state information, and commands are fed as input to the symbolic model, and quantitative sensor data is input to a simplified physical model of the system. These modules are designed to leverage existing system models, which can be high or low fidelity. The symbolic model aids signal-based analysis in terms of mode selection or other discrete outputs. The physical model improves sensitivity through separation of predictable and unpredictable signal components.

Time-varying quantities are analyzed in two groups: (1) signals with a high degree of correlation to others, or signals that are not isolated in a diagnostic sense, are passed to the coherence-analysis component of BEAM; (2) signals that may uniquely indicate a fault, as well as those already suspected to be faulty, are passed through



This **BEAM Architecture** expands upon the original BEAM formulation in the following respects: (1) incorporation of physical models, (2) integration of symbolic reasoning components, (3) statistical and stochastic modeling of individual signals (augmenting or supplanting prior wavelet-based modeling), (4) trending to failure for individual signals and cross-signal features, and (5) enumeration of results using an expert system.

feature-extraction components. This split allows BEAM to consider very complex faults in the system, including interference faults or miscommunication that escape univariate detection methods, while retaining robustness in poorly redundant systems or in the face of gross nonlinearity. The components of BEAM described in the figure are summarized as follows:

- The model filter combines sensor data with predictions from a real-time physical model. The inclusion of physical models, where available, is the most efficient way to incorporate domain knowledge into signal-based data analysis.
- The symbolic data model interprets status variables and commands to provide an accurate, evolving picture of the system mode and requested actions.
- The coherence-based fault detector tracks the cobehavior of temporally varying quantities to expose changes in internal operating physics.

- The dynamical invariant anomaly detector tracks parameters of individual signals to sense subtle deviations and predict near-term behavior.
- The Informed Maintenance Grid (IMG) studies evolution of cross-channel behavior over the medium- and long-term operation of the system. It tracks consistent subthreshold deviations and exposes deterioration and loss of performance.
- The prognostic assessment yields a forward projection of individual signals, based upon their extracted parameters. It also provides a useful short-term assessment of impending faults and loss of functionality.
- The causal system model is a rule-based connectivity model designed to improve isolation of fault sources and identification of actor signals.
- The interpretation layer collates observations from all separate components and submits a single fault report in a

format useable by recovery software, planners or other AI software, and/or human operators.

*This work was done by Ryan Mackey, Mark James, Han Park, and Michail Zak of Caltech for NASA's Jet Propulsion Laboratory. Further information is contained in a TSP [see page 1].*

*In accordance with Public Law 96-517, the contractor has elected to retain title to this invention. Inquiries concerning rights for its commercial use should be addressed to Technology Reporting Office*

*JPL*

*Mail Stop 249-103  
4800 Oak Grove Drive  
Pasadena, CA 91109  
(818) 354-2240*

*Refer to NPO-21126, volume and number of this NASA Tech Briefs issue, and the page number.*

## Determining Direction of Arrival at a Y-Shaped Antenna Array

The direction is computed from differences among times of arrival of signals.

An algorithm computes the direction of arrival (both azimuth and elevation angles) of a lightning-induced electromagnetic signal from differences among the times of arrival of the signal at four antennas in a Y-shaped array on the ground. In the original intended application of the algorithm, the baselines of the array are about 90 m long

and the array is part of a lightning-detection-and-ranging (LDAR) system. The algorithm and its underlying equations can also be used to compute directions of arrival of impulsive phenomena other than lightning on arrays of sensors other than radio antennas: for example, of an acoustic pulse arriving at an array of microphones.

The underlying equations express the differences among the times of arrival as functions of the inner products of (1) the unit vector of the direction of arrival and (2) the unit vectors along the baselines of the array. To obtain a solution for the unit vector (and thus, equivalently, the azimuth and elevation angles) of the direction of arrival,

*John F. Kennedy Space  
Center, Florida*

the underlying equations are combined and modified into a matrix formulation that is amenable to a least-squares solution.

The value of the inner product calculated from the measured difference between the times of arrival of the signal at the two antennas on each baseline specifies a circle in the sky upon which nominally lies the apparent point in the sky from which the signal came. Thus, from the time-of-arrival measurements on all three baselines of the Y-shaped array, it is possible to specify three circles in the sky, all of which nominally contain the apparent point in the sky from which the signal came. Nominally, all three circles would intersect at a single point in the sky corresponding to the direction of arrival. In practice, random measurement errors prevent the three circles from intersecting at a single

point; instead, they intersect to define a small triangle-like patch of sky. The least-squares-error solution corresponds to a point near the triangle, such that sum of squares of distances between the solution point and each circle in the sky is the least possible value.

This algorithm has been verified on both synthetic data and measurement data recorded by a prototype short-baseline LDAR system. An analysis of errors revealed that the azimuth error depends only on elevation and that the elevation error is small except near the horizon. Further analysis showed that the addition of a vertical baseline (two additional antennas mounted on the top and bottom of a tower) would add little of value to the measurements and calculations since the LDAR source points are typically above 20° elevation.

The primary source of error in the algorithm is the simplifying assumption that the signal originates at an infinite distance. While this assumption is never strictly true, it provides an acceptable approximation as long as the distance of the signal source is much greater than the length of the baselines. The least-squares approach also reduces this error.

An additional equation that takes account of the curvature of a wavefront arriving from a source at a finite distance has been derived and found to be accurate at close range. An algorithm that would solve iteratively for azimuth, elevation, and range of the source has been proposed but not tested.

*This work was done by Stan Starr of Kennedy Space Center. Further information is contained in a TSP [see page 1]. KSC-12059*

## Self-Supervised Dynamical Systems

Mathematical models describe coupled motor and mental dynamics.

Some progress has been made in a continuing effort to develop mathematical models of the behaviors of multi-agent systems known in biology, economics, and sociology (e.g., systems ranging from single or a few biomolecules to many interacting higher organisms). This effort at an earlier stage was reported in "Characteristics of Dynamics of Intelligent Systems" (NPO-21037), *NASA Tech Briefs*, Vol. 26, No. 12 (December 2002), page 48.

To recapitulate from the cited prior article: Living systems can be characterized by nonlinear evolution of probability distributions over different possible choices of the next steps in their motions. One of the main challenges in mathematical modeling of living systems is to distinguish between random walks of purely physical origin (for instance, Brownian motions) and those of biological origin. Following a line of reasoning from prior research, it has been assumed, in the present development, that a biological random walk can be represented by a nonlinear mathematical model that represents coupled mental and motor dynamics incorporating the psychological

concept of reflection or self-image. The nonlinear dynamics impart the lifelike ability to behave in ways and to exhibit patterns that depart from thermodynamic equilibrium. Reflection or self-image has traditionally been recognized as a basic element of intelligence.

The nonlinear mathematical models of the present development are denoted self-supervised dynamical systems. They include (1) equations of classical dynamics, including random components caused by uncertainties in initial conditions and by Langevin forces, coupled with (2) the corresponding Liouville or Fokker-Planck equations that describe the evolutions of probability densities that represent the uncertainties. The coupling is effected by fictitious information-based forces, denoted supervising forces, composed of probability densities and functionals thereof.

The equations of classical mechanics represent motor dynamics — that is, dynamics in the traditional sense, signifying Newton's equations of motion. The evolution of the probability densities represents mental dynamics or self-image. Then the interaction between the physi-

*NASA's Jet Propulsion Laboratory,  
Pasadena, California*

cal and mental aspects of a monad is implemented by feedback from mental to motor dynamics, as represented by the aforementioned fictitious forces. This feedback is what makes the evolution of probability densities nonlinear. The deviation from linear evolution can be characterized, in a sense, as an expression of free will.

It has been demonstrated that probability densities can approach prescribed attractors while exhibiting such patterns as shock waves, solitons, and chaos in probability space. The concept of self-supervised dynamical systems has been considered for application to diverse phenomena, including information-based neural networks, cooperation, competition, deception, games, and control of chaos. In addition, a formal similarity between the mathematical structures of self-supervised dynamical systems and of quantum-mechanical systems has been investigated.

*This work was done by Michail Zak of Caltech for NASA's Jet Propulsion Laboratory. Further information is contained in a TSP [see page 1]. NPO-30634*





## Life Sciences

### Hardware, Techniques, and Processes

- 53 Hydrofocusing Bioreactor for Three-Dimensional Cell Culture
- 54 Species Specific Bacterial Spore Detection Using Lateral-Flow Immunoassay With DPA-Triggered Tb Luminescence
- 55 Live/Dead Bacterial Spore Assay Using DPA-Triggered Tb Luminescence
- 56 Growth Conditions To Reduce Oxalic Acid Content of Spinach



## Hydrofocusing Bioreactor for Three-Dimensional Cell Culture

Hydrofocusing reduces shear while “herding” cells and air bubbles.

Lyndon B. Johnson Space Center,  
Houston, Texas

The hydrodynamic focusing bioreactor (HFB) is a bioreactor system designed for three-dimensional cell culture and tissue-engineering investigations on orbiting spacecraft and in laboratories on Earth. The HFB offers a unique hydrofocusing capability that enables the creation of a low-shear culture environment simultaneously with the “herding” of suspended cells, tissue assemblies, and air bubbles. Under development for use in the Biotechnology Facility on the International Space Station, the HFB has successfully grown large three-dimensional, tissue-like assemblies from anchorage-dependent cells and grown suspension hybridoma cells to high densities.

Conventional bioreactors rely on agitation to suspend cells and attachment materials and to facilitate the mass transfer required for the growth of cells and tissue assemblies. However, the shear force generated by agitation, can affect cell-cell interactions and degrade three-dimensional tissue development. Johnson Space Center has developed rotating-wall perfused-system (RWPS) bioreactors that create low-shear culture environments and support three-dimensional tissue development. However, their ability to control the locations of cells and tissue aggregates within vessels is limited. Moreover, air bubbles that form within the culture media in the vessels cannot be removed, although such removal is critical for operation in orbit around the Earth.

The HFB, based on the principle of hydrodynamic focusing, provides the capability to control the movement of air bubbles and removes them from the bioreactor without degrading the low-shear culture environment or the suspended three-dimensional tissue assemblies. The HFB also provides unparalleled control over the locations of cells and tissues within its bioreactor vessel during operation and sampling.

The HFB includes a rotating, dome-shaped cell-culture vessel with a centrally located sampling port and an internal rotating viscous spinner attached to a rotating base (see Figure 1). The vessel and viscous spinner can rotate at the same speed or different speeds and directions to create the desired levels of hydrodynamic force within the vessel. Both the low-shear suspension of cells and control of the locations of cells and air bubbles are effected by means of the hydrodynamic force created by the flow within the vessel and fluid drag along the surface of the viscous spinner. A gas-per-

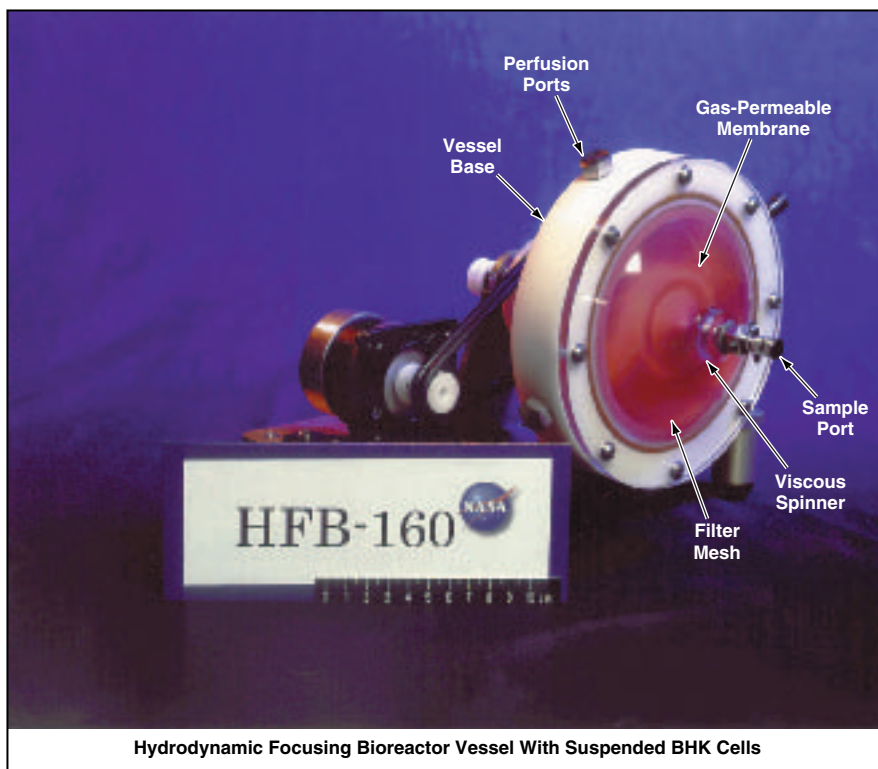


Figure 1. The **Hydrodynamic Focusing Bioreactor** utilizes rotation and viscosity to generate hydrodynamic forces for controlling locations of cells and bubbles while maintaining low shear.

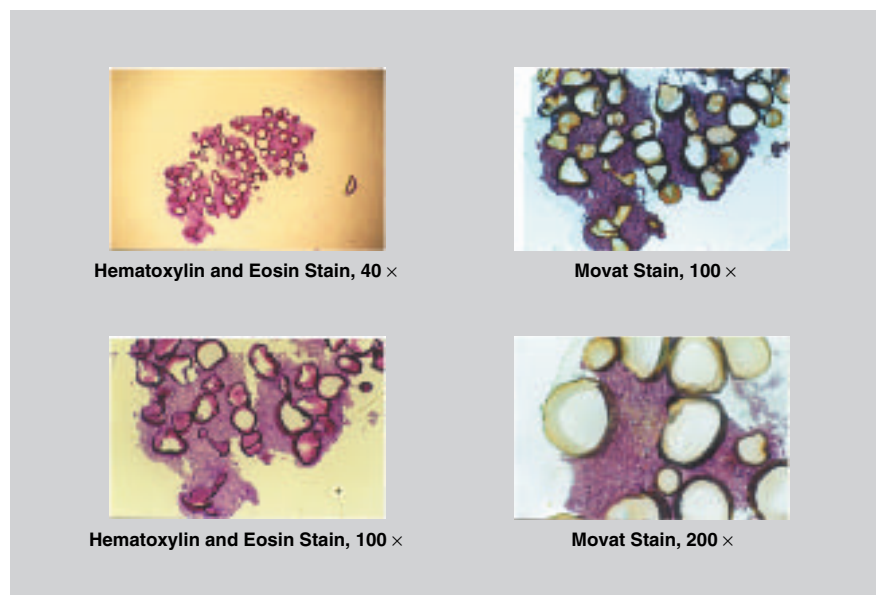


Figure 2. **Aggregates of Baby-Hamster Kidney Cells** grown in the HFB during ten-day intervals were photographed at two different magnifications after histological staining.

meable membrane connected to the base of the vessel enables the exchange of gas between the medium in the vessel and an incubator environment in which the vessel is

placed. Average shear values of 0.001 dynes per square centimeter were estimated for a rotation rate of 10 rpm — a rate at which efforts to suspend large, three-

dimensional, tissue-like assemblies have been successful.

Anchorage-dependent cells, including primary cells, transformed cells, genetically engineered cells and cell lines, and suspension hybridoma cells were successfully cultured either as mono- or co-cultures in the HFB for times as long as 2 weeks. Cultures were initiated by inoculating cells, variously with or without attachment materials, into the vessel through the sampling port, filling the vessel completely with a culture medium, and setting rotation rates to maintain suspension. Large three-dimensional, tis-

suelike assemblies were obtained from HFB cultures of anchorage-dependent cells (see Figure 2). In addition, critical stages in three-dimensional, tissue-like growth (cell attachment, three-dimensional aggregation, and formation of an extracellular matrix) were observed with all anchorage-dependent cells cultured in the HFB.

This work was done by Steve R. Gonda and Glenn F. Spaulding of **Johnson Space Center**, Yow-Min D. Tsao, Scott Flechsig and Leslie Jones of **Wyle Laboratories**, and Holly Soehnge of **Universities Space Research Associates**.

Title to this invention, covered by U.S. Patent No. 6,001,642 has been waived under the provisions of the National Aeronautics and Space Act {42 U.S.C. 2457 (f)}. Inquiries concerning licenses for its commercial development should be addressed to

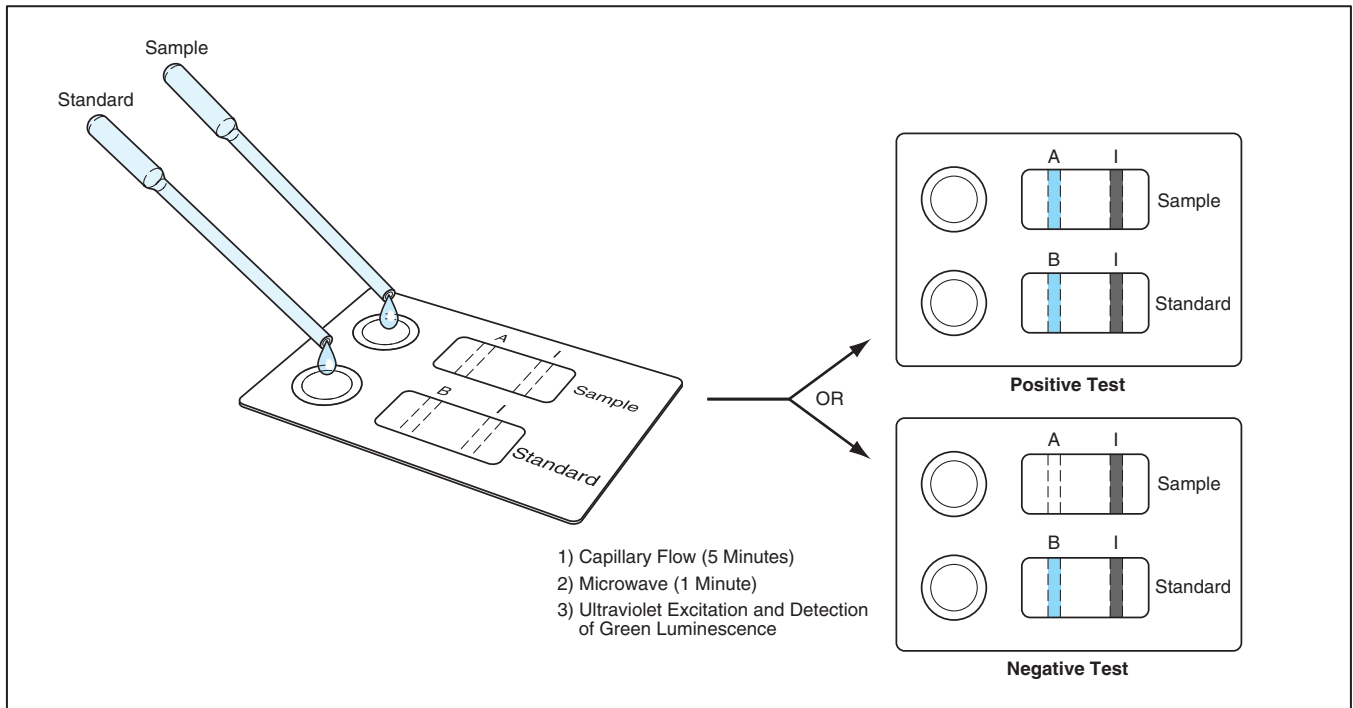
Wyle Laboratories  
1290 Hercules Drive  
Suite 120  
Houston, TX 77058

Refer to MSC-22538, volume and number of this NASA Tech Briefs issue, and the page number.

## Species Specific Bacterial Spore Detection Using Lateral-Flow Immunoassay With DPA-Triggered Tb Luminescence

A highly-sensitive assay can be performed in minutes.

NASA's Jet Propulsion Laboratory,  
Pasadena, California



**An Assay Is Performed** on a sample suspected of containing bacterial spores of a species of interest, in parallel with an assay of a standard containing a known concentration of *Bacillus subtilis*. The intensity of luminescence in region A under ultraviolet illumination is proportional to the number density of the spores.

A method of detecting bacterial spores incorporates

- A method of lateral-flow immunoassay in combination with
- A method based on the luminescence of Tb<sup>3+</sup> ions to which molecules of dipicolinic acid (DPA) released from the spores have become bound.

The second-mentioned component method, denoted the method of DPA-triggered Tb luminescence, was described

in somewhat more detail as a precursor of a related development reported in "Improved Technique for Detecting Endospores via Luminescence" (NPO-21240) *NASA Tech Briefs*, Vol. 26, No. 7 (July 2002), page 56.

The present combination of lateral-flow immunoassay and DPA-triggered Tb luminescence was developed as a superior alternative to a prior lateral-flow immunoassay method in which detection involves the

visual observation and/or measurement of red light scattered from colloidal gold nanoparticles. The advantage of the present combination method is that it affords both

- High selectivity for spores of the species of bacteria that one seeks to detect (a characteristic of lateral-flow immunoassay in general) and
- Detection sensitivity much greater (by virtue of the use of DPA-triggered Tb luminescence instead of gold nanoparticles) than

that of the prior lateral-flow immunoassay method. The sensitivity afforded by the present method is so much greater that whereas the previously reported detection limit of lateral-flow immunoassay was  $10^5$  spores/mL, the estimated detection limit of the present method is 100 spores/mL.

DPA in a 1:1 complex with  $\text{Ca}^{2+}$  ions is present in high concentration in bacterial spores, and has not been observed in any lifeforms other than bacterial spores. Hence, DPA is an indicator molecule for the presence of bacterial spores. Fortuitously, DPA is also a classic inorganic-chemistry ligand that binds metal ions with high affinity. When bound to  $\text{Tb}^{3+}$  ions, DPA triggers intense green luminescence of the ions under ultraviolet excitation. The intensity of the luminescence can be correlated with the number density of bacterial spores per milliliter. Moreover, the concentrations of compounds that could potentially give rise to spurious luminescence are typically much smaller than the concentration of DPA, and the strengths with which they bind to  $\text{Tb}^{3+}$  are of the order of a millionth of that of DPA, so that the desired luminescence signal appears against a dark background.

The figure summarizes the steps of the

present method. A sample suspected of containing bacterial spores is prepared by suspending raw sample material in an aqueous solution that contains  $\text{Tb}^{3+}$  ions. A volume of  $\approx 100 \mu\text{L}$  of the sample is placed on a test strip — a nitrocellulose membrane on which species-specific antibodies are bound in an area denoted the sample region (area A in the figure). Capillary action moves the spores along the strips. In the sample region, specific binding of membrane-bound antibodies captures and immobilizes the bacterial spores. Next, the strip is exposed to microwave power to release DPA from the spores. The released DPA binds to the  $\text{Tb}^{3+}$  ions in the solution. Hence, when the strip is exposed to ultraviolet light, the  $\text{Tb}^{3+}$  ions luminesce green, signaling the presence of the bacterial spores from which the DPA was released.

At the same time, a volume of  $\approx 100 \mu\text{L}$  of a similar solution containing a known concentration of *Bacillus subtilis*, to be used as a standard, is placed on a similarly prepared, parallel membrane denoted the standard strip, which includes an antibody-coated area designated the standard region (area B in the figure). The standard strip is subjected to the same process as is the test

strip. A combination of green luminescence from the region B and a change in color in regions I of both strips indicates that the assay has worked properly. In that case, the ratio of between the intensity of luminescence in region A and that in region B is proportional to the number density of bacterial spores in the sample. The entire assay can be performed in 10 minutes or less.

*This work was done by Adrian Ponce of Caltech for NASA's Jet Propulsion Laboratory. Further information is contained in a TSP [see page 1].*

*In accordance with Public Law 96-517, the contractor has elected to retain title to this invention. Inquiries concerning rights for its commercial use should be addressed to Intellectual Assets Office*

*JPL*

*Mail Stop 202-233*

*4800 Oak Grove Drive*

*Pasadena, CA 91109*

*(818) 354-2240*

*E-mail: ipgroup@jpl.nasa.gov*

*Refer to NPO-30469, volume and number of this NASA Tech Briefs issue, and the page number.*

## Live/Dead Bacterial Spore Assay Using DPA-Triggered Tb Luminescence

A relatively simple procedure can be executed in about 20 minutes.

A method of measuring the fraction of bacterial spores in a sample that remain viable exploits DPA-triggered luminescence of  $\text{Tb}^{3+}$  and is based partly on the same principles as those described in the immediately preceding article. Unlike prior methods for performing such live/dead assays of bacterial spores, this method does not involve counting colonies formed by cultivation (which can take days), or counting of spores under a microscope, and works whether or not bacterial spores are attached to other small particles (i.e., dust), and can be implemented on a time scale of about 20 minutes.

Like the method of the preceding article, this method exploits the facts that (1) DPA is present naturally only in bacterial spores; (2) when bound to  $\text{Tb}^{3+}$  ions, DPA triggers intense green luminescence of the ions under ultraviolet excitation; and (3) the intensity of the luminescence can be correlated with the concentration of DPA released from

spores and, thus, with the number density of the spores. It has been found that in the case of a sample comprising bacterial spores suspended in a solution, the DPA can be released from the viable spores into the solution by using L-alanine to make them germinate. It has also been found that by autoclaving, microwaving, or sonicating the sample, one can cause all the spores (non-viable as well as viable) to release their DPA into the solution. When the released DPA binds  $\text{Tb}^{3+}$  ions in the solution and the sample is exposed to ultraviolet light, the solution luminesces, as described in the preceding article.

Therefore, in this method, one divides a sample into two parts. For the first part, germination is used to release the DPA from the viable spores; for the second part, one of the three other techniques is used to release DPA from all the spores. The intensities of the DPA-triggered luminescence of both parts of the sample are measured. Then the frac-

*NASA's Jet Propulsion Laboratory,  
Pasadena, California*

tion of viable spores is calculated as the ratio between the measured luminescence intensities of the first and second parts of the sample.

*This work was done by Adrian Ponce of Caltech for NASA's Jet Propulsion Laboratory. Further information is contained in a TSP [see page 1].*

*In accordance with Public Law 96-517, the contractor has elected to retain title to this invention. Inquiries concerning rights for its commercial use should be addressed to*

*Intellectual Assets Office*

*JPL*

*Mail Stop 202-233*

*4800 Oak Grove Drive*

*Pasadena, CA 91109*

*(818) 354-2240*

*E-mail: ipgroup@jpl.nasa.gov*

*Refer to NPO-30444, volume and number of this NASA Tech Briefs issue, and the page number.*

---

## Growth Conditions To Reduce Oxalic Acid Content of Spinach

A controlled-environment agricultural (CEA) technique to increase the nutritive value of spinach has been developed. This technique makes it possible to reduce the concentration of oxalic acid in spinach leaves. It is desirable to reduce the oxalic acid content because oxalic acid acts as an anti-nutritive calcium-binding component. More than 30 years ago, an enzyme (an oxidase) that breaks down oxalic acid into CO<sub>2</sub> and H<sub>2</sub>O<sub>2</sub> was discovered and found to be naturally present in spinach leaves. However, nitrate, which can also be present

because of the use of common nitrate-based fertilizers, inactivates the enzyme. In the CEA technique, one cuts off the supply of nitrate and keeps the spinach plants cool while providing sufficient oxygen. This technique provides the precise environment that enables the enzyme to naturally break down oxalate. The result of application of this technique is that the oxalate content is reduced by 2/3 in one week.

*This work was done by Corinne Johnson-Rutzke of Cornell Research Foundation, Inc., for **Kennedy Space Center**.*

*In accordance with Public Law 96-517, the contractor has elected to retain title to this invention. Inquiries concerning rights for its commercial use should be addressed to*

*John Brenner*

*Cornell Research Foundation*

*20 Thornwood Drive, Suite 105*

*Ithaca, NY 14850*

*Tel. No.: (607) 257-1081*

*E-mail: jbff@cornell.edu*

*Refer to KSC-12240, volume and number of this NASA Tech Briefs issue, and the page number.*



National Aeronautics and  
Space Administration

